sensors

MDPI

Review

Nanozymes—Hitting the biosensing "target"

Yingfen Wu[1], Diane C. Darland[2,*], and Julia Xiaojun Zhao[1,*]

[1] Department of Chemistry, University of North Dakota, Grand Forks, ND 58202, United states; yingfen.wu@und.edu; julia.zhao@und.edu.
[2] Department of Biology, University of North Dakota, Grand Forks, ND 58202, United States; diane.darland@und.edu.
* Correspondence: julia.zhao@und.edu; diane.darland@und.edu; Tel.: +01-701-777-3610 (JXZ); +01-701-777-4597 (DCD).

Abstract: Nanozymes are a class of artificial enzymes that have dimensions in the nanometer range and can be composed of simple metal and metal oxide nanoparticles, metal nanoclusters, dots (both quantum and carbon), nanotubes, nanowires, or multiple metal-organic frameworks (MOFs). They exhibit excellent catalytic activities with low cost, high operational robustness, and a stable shelf-life. More importantly, they are amenable to modifications that can change their surface structures and increase the range of their applications. There are three main classes of nanozymes including the peroxidase-like, the oxidase-like, and the antioxidant nanozymes. Each of these classes catalyzes a specific group of reactions. With the development of nanoscience and nanotechnology, the variety of applications for nanozymes in diverse fields has expanded dramatically, with the most popular applications in biosensing. Nanozyme-based novel biosensors have been designed to detect ions, small molecules, nucleic acids, proteins, and cancer cells. The current review focuses on the catalytic mechanism of nanozymes, their application in biosensing, and the identification of future directions for the field.

Keywords: nanozyme; biosensing; catalytic activity

Citation:

Academic Editor: Firstname Lastname

Received: date
Accepted: date
Published: date

1. Introduction

Enzymes are biocatalysts that accelerate chemical reactions of many metabolic processes in cells. While they are generally globular proteins, and a few contain nucleic acids, they tend to act alone or in larger functional complexes. The catalytic activity of the enzyme is generally determined by the structure which is specified by the primary amino acid sequence. Usually, the size of the enzyme is larger than the substrate(s), which typically binds in specific active sites determined by the primary, secondary and tertiary structure of proteins in the complex [1]. Enzymes are generally specific to their substrates and reduce the activation energy required to complete the reaction. Because of the properties inherent in the primary, secondary, tertiary and quaternary structures, enzymes are limited to functional ranges in temperature, pH, and salinity compared with industrial catalysts such as ethylene oxide [2]. Despite their functional range limitations, enzymes have tremendous application potential as biocatalysts. Several technologies have been able to address many structural and functional shortcomings of enzymes such as low operational stability, sensitivity to operational environments, high cost of production, purification quality consistency, and cycling optimization. However, many challenges still remain with regard to effective utilization of biocatalysts in biosensing, including simultaneous discrimination of multiple targets. The combination of biocatalysts with nanotechnology offers an opportunity to address these challenges effectively.

With recent, rapid developments in nanotechnology, nanozymes have attracted significant interest due to their novel and starkly distinct potential when compared with the bulkier, amino acid-based counterparts. Nanozymes are nanomaterials which display

enzyme-like properties and can catalyze reactions [3]. These include nanomaterials such as simple metal and metal oxide nanoparticles [4,5], metal nanoclusters [6], quantum dots and carbon dots [7,8], nanotubes and nanowires [9,10], as well as metal-organic frameworks (MOFs) [11]. These diverse nanomaterials can exhibit catalytic capabilities similar to enzymes, but can overcome many of the effective range and stability limitations associated with enzymes. The advantageous features of nanozymes include low cost of production, high catalytic activity, high operational robustness, long shelf-life, and ease of generating modifications [12,13]. Also, because of their inherent properties, nanozymes can work as recognition receptors [14] or signal tags [15]. Furthermore, they can be used as signal amplifiers via utilization of different detection methods such as electrochemistry [16], fluorescence [17], colorimetry [18], immunoassay [19], and other analysis approaches [20]. Nanozymes have recently been utilized in a broad array of applications including biosensing [21], environmental protection [22], antibacterial application [23], cancer therapy [24], and cryoprotection [25].

The primary goals of this review are to (1) describe the different types of nanozymes and their functional elements; (2) define their catalytic mechanisms, including limitations; and (3) identify current and future applications for biosensing from ions to tissues (Figure 1).

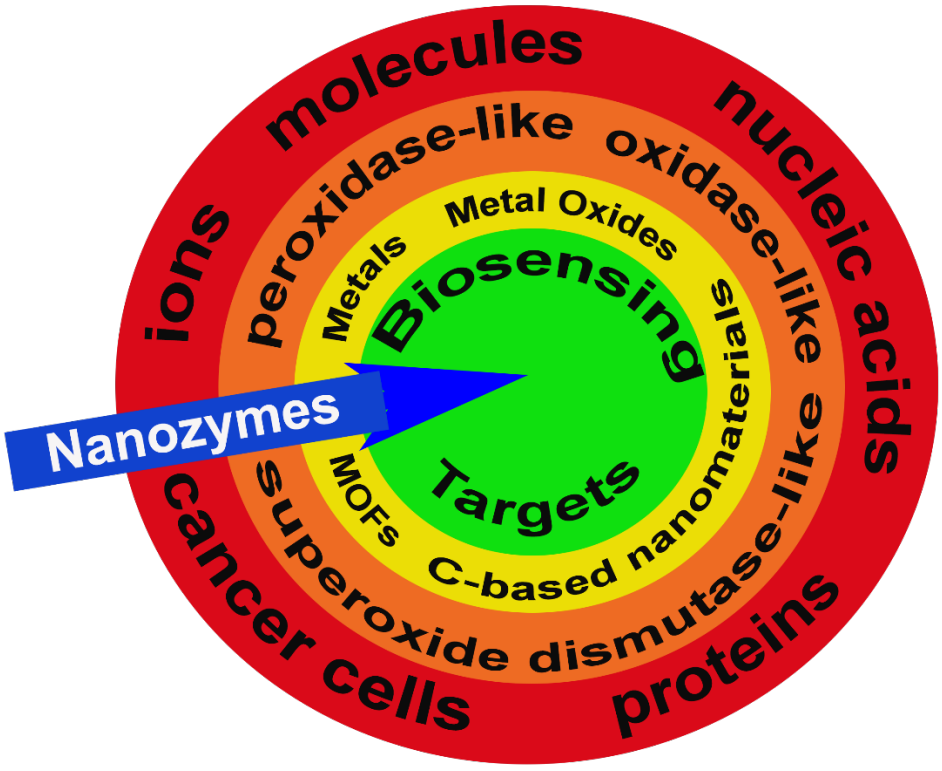

Figure 1. Nanozymes and biosensing targets. Examples of potential targets for nanozymes (blue arrow) including ions, molecules, nucleic acids, proteins, and cancer cells (red band). There are three categories of nanozymes grouped by their functional enzyme-mimicking capacity including, peroxidase-like, oxidase-like, and superoxide dismutase-like (orange band) with the active sites generated by metals, metal oxides, metal-organic frameworks (MOFs), and carbon (C)-based nanomaterials (yellow band). Collectively, these features attract and facilitate the enzymatic reaction at the nanozyme target biosensing target (green circle).

2. Nanozyme classification and their catalytic mechanisms

Currently, more than 40 types of nanozymes have been reported. All of them embody the same basic framework; they are made of nanomaterials with specific nanostructures able to catalyze biochemical reactions of specific substrates, although the mechanisms are not necessarily comparable to natural enzymes. Nanozymes also show similar enzymatic kinetics and catalytic mechanisms comparable to those displayed by natural enzymes. Based on

the activities they exhibit, nanozymes are categorized into two large families: the oxidoreductase family and the hydrolase family. The members of the oxidoreductase family are involved in redox catalysis and function similarly to catalase, superoxide dismutase, oxidase, peroxidase, or nitrate reductase. Members of the hydrolase family are involved in catalyzing hydrolysis reactions in a fashion similar to phosphatase, protease, nuclease, esterase, or silicatein [26]. The major groups are further subdivided below based on the active component of the nanozyme and a comprehensive list of groups, their mechanisms of action, major targets, and detection mechanisms is provided in Table 1.

2.1. Nanozyme active component

2.1.1. Metal elements

Many metals have enzymatic activity, primarily based on their atomic structure and valence properties, that promote the generation of reactive oxygen species (ROS) and facilitate the electron-transfer process. Noble metals such as gold (Aurum, Au), silver (Argentum, Ag), bismuth (Bi), palladium (Pd) and platinum (Pt) display unique plasmonic features at the nanoscale level, one of which is their large optical enhancement. This is also referred to as the surface plasmon resonance (SPR) [27], which is a phenomenon of the plasma resonance resulting in radiant light emission, caused by the resonant oscillation of the free electrons in the presence of light. As a result, for example, Au nanoparticles (NPs) have been designed and applied to different fields, including biosensing, dark-field imaging, and nanomedicine [28-30]. Au NPs (positively charged) have been effectively utilized as natural peroxidase mimics for detection of hydrogen peroxide (H_2O_2) and glucose in the presence of 3,3′,5,5′-tetramethylbenzidine (TMB) [31]. For example, over a broad dynamic pH range, a folic acid graphene oxide-Au nanocluster hybrid (GFA) has been used to conduct quantitative colorimetric detection of folate receptor on human cervical (HeLa) and breast cancer (MCF-7) cells [32]. The mechanism involves the catalyzation of TMB and H_2O_2 by GFA based on its enzyme mimicking activity [32]. Further, Au NPs have been used to detect target DNA or microRNA (miRNA) using complementary nucleic acids immobilized on Au NPs which then facilitated hybridization of the nucleic acids [33,34]. Au NPs also have been used to detect ions and cancer cells [35,36] further supporting the value of this nanozyme in biological applications.

2.1.2. Metal oxides

The catalytic activities of the metal oxides are comparable to those of the metal ions, with the exception of the noble metal elements. The metal oxides in NPs will work as metal ions when combined with H_2O_2 because of their different valence values.

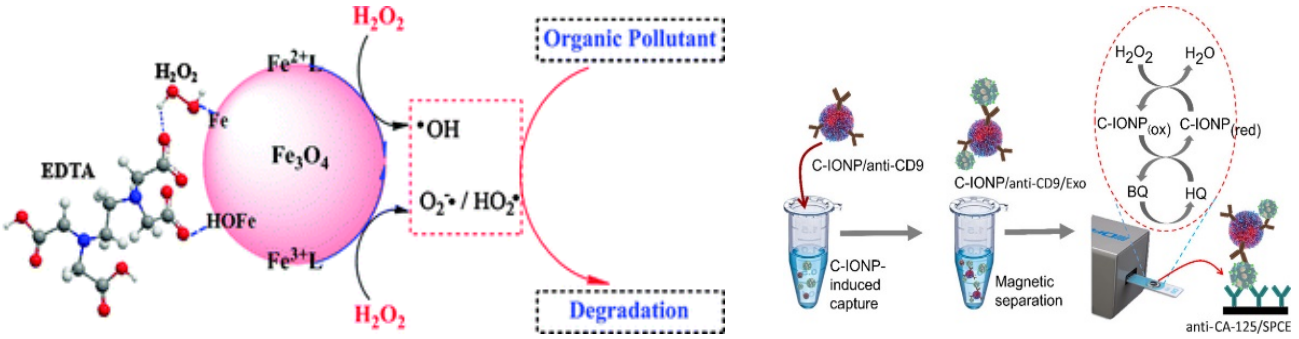

(**a**) (**b**)

Fe oxides nanozymes

The nanomaterials with iron ions work as peroxidase mimics, generally functioning via a Fenton reaction as advanced oxidation processes (AOPs). Iron oxide-based nanoparticles, including the ferromagnetic (Fe_3O_4) NPs, and hematite (Fe_2O_3) NPs (Figure 2) have a variety of applications based on the partner with which they are combined. They work as a peroxidase when combined with H_2O_2, or function as an oxidase when serving as a glucose sensor. Further, they act as a dual biocatalyst when utilizing a pH-dependent mechanism to display peroxidase and catalase functional potential. Figure 2 illustrates the use of ferromagnetic and hematite products in combination with H_2O_2 to target organic pollutants for degradation (Figure 2a) or to detect exosomes (Figure 2b). The fundamental reaction series is depicted in equation 1-7 [37]. The H_2O_2 combines with ferrous (Fe^{2+}) ions to generate hydroxyl radicals via a complex reaction sequence. Ferric (Fe^{3+}) ions also react with H_2O_2. This reaction has many advantages such as a low level of iron ion leaching, the efficient cycling of iron ions, low iron sludge production, the wide working pH range, and the reusability as well as the long term stability of the catalysts [37]. In this way, the iron oxide-based nanomaterials react with or catalyze H_2O_2 and can be applied in H_2O_2-based reactions. Additionally, the sulfide analogs of magnetite, like greigite (Fe_3S_4), which shows the same inverse spinel structure as its oxide counterpart Fe_3O_4, exhibits peroxidase-like activity, similar to Fe_3O_4 [38]. Based on the different valence status, the other Fe-containing nanoparticles like ferric hexacyanoferrate, Prussian Blue (PB) [39], or magnetic nanoparticles [40] show similar enzyme-like properties.

$$Fe^{2+} + H_2O_2 \rightarrow Fe^{3+} + HO\cdot + OH^{\ominus} \quad (1)$$

$$Fe^{3+} + H_2O_2 \rightarrow Fe^{2+} + HO_2\cdot + H^{\oplus} \quad (2)$$

$$H_2O_2 + HO\cdot \rightarrow HO_2\cdot + H_2O \quad (3)$$

$$HO_2\cdot \rightarrow O_2^{\cdot -} + H^{\oplus} \quad (4)$$

$$Fe^{3+} + HO_2\cdot \rightarrow Fe^{2+} + O_2 + H^{\oplus} \quad (5)$$

$$Fe^{3+} + O_2^{\cdot -} \rightarrow Fe^{2+} + O_2 \quad (6)$$

$$Fe^{2+} + HO\cdot + H^{\oplus} \rightarrow Fe^{3+} + HO_2 \quad (7)$$

Figure 2. Examples of iron (Fe)-based metal oxide nanozymes. The figure depicts catalysis reactions of H_2O_2 decomposition reaction with Fe_3O_4 or Fe_2O_3 [41] NPs. (a) The Fe_3O_4 NPs bear active H_2O_2 on their surface that generate ROS and, therefore, increase the degradation rates of organic pollutants such as pentachlorophenol, sulfamonomethoxine, and Rhodamine B (RhB). Reprinted from [42] with permission from Royal Society of Chemistry. EDTA: Ethylenediaminetetraacetic acid. (b) Peroxidase-mimicking activity of the carboxyl group-functionalized iron oxide nanoparticles (C-IONPs) displayed the ability to catalyze

oxidation of TMB in the presence of H_2O_2 for the direct isolation and quantification of disease-specific exosomes, as the authors demonstrated using exosomes bearing the ovarian cancer biomarker (CA-125). Reprinted with permission from [41]. Exo: exosomes; SPCEs: screen-printed carbon electrodes; HQ: hydroquinone; BQ: benzoquinone.CD9: tetraspainin-9; CA-125: cancer antigen 125. Copyright (2021), from the American Chemical Society.

Other metal oxides-based nanozymes

Due to their valence properties and outer orbital ring structure, some ions, particularly the transition metals, have multiple oxidation states which gives them the ability to generate the Fenton-like reaction. Therefore, a specific oxidation state of an ion can be regenerated from an inactive state through a simple redox cycle. In this way, many metal ions such as chromium (Cr) [43], cobalt (Co) [44], copper (Cu) [45], manganese (Mn) [46], and ruthenium (Ru) [47], to name a few, react with H_2O_2 in a Fenton-like way (Figure 3), with the end result of catalysis of H_2O_2.

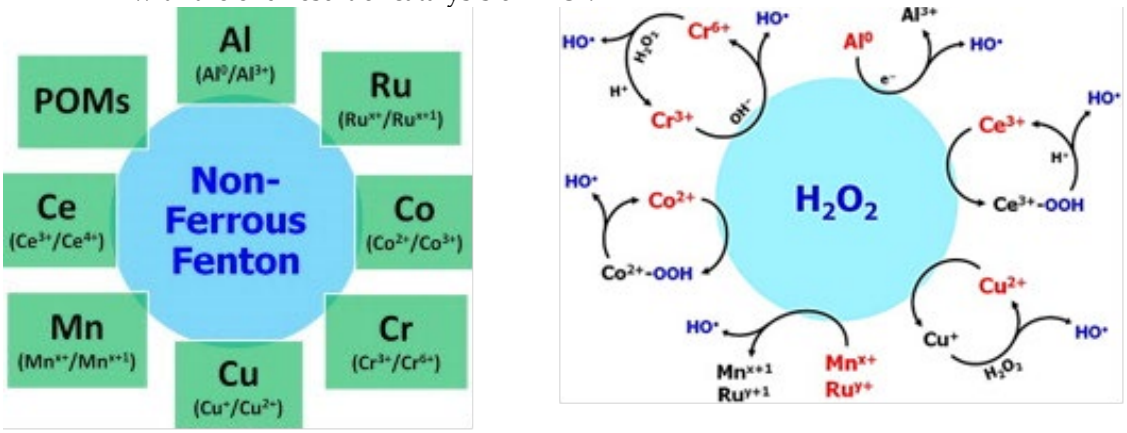

Figure 3. Non-ferrous Fenton ions and their reaction with hydrogen peroxide. (a) A schematic is shown that highlights non-Ferrous Fenton ions with the oxidation states that catalyze the substrates [48]. Polyoxometalates (POMs) are the metal oxyanion clusters. (b) This schematic depicts an overview of the redox reactions between H_2O_2 and various non-ferrous Fenton catalysts. The species highlighted in red or blue indicate the active Fenton catalyst and the product, respectively. Reprinted from [48], with permission from Elsevier.

Mn oxide nanozymes

Manganese exists in various oxidation states ranging from 0 to +7; however, only the oxidation states of +2 to +4 have catalytic significance [49]. The reason is that only Mn^{2+} and Mn^{4+} are stable in the aquatic environment which is critical for bioapplications. The facile interconversion between Mn^{2+} and Mn^{4+} via Mn^{3+} ensures that the process of Mn-catalyzed Fenton-like activation of H_2O_2 is rapid and efficient. Usually, all Mn ions occur as oxide polymorphs (MnO, Mn_3O_4, MnOOH and MnO_2), and when they are "doped" or incorporated into NPs they react efficiently with H_2O_2 [50-53]. However, there are caveats associated with the different oxidation states for Mn in that physical form, since chemical composition and concentration can generate different ROS, including HO· and superoxide ($O_2^{\cdot-}$) which are highly cytotoxic.

Cu oxide nanozymes

Another potent nanozyme involves Cu ions, when combined with H_2O_2, which shows redox properties similar to iron. Cu ions have two oxidation states, Cu^{2+} and Cu^{+}, both of which can react with H_2O_2 easily, similar to the way in which Fe^{3+} and Fe^{2+} react with H_2O_2 [54,55]. The difference lies in the fact that in acidic and near-neutral conditions, Cu^{+} reacts with H^{+} and generates Cu^{2+}, which reduces the effective Cu^{+} available to react with H_2O_2. As a result, the pH value of the solution needs to be corrected before the nanozyme "sensing" process starts (Figure 4).

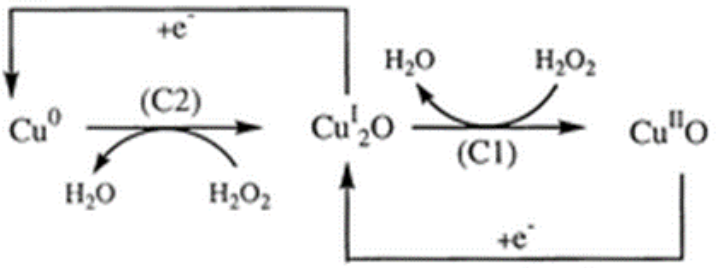

Figure 4. **The copper (Cu)-mediated reduction process of H_2O_2 at the CuSPE** (copper-plated screen-printed carbon electrode) [56]. The transition from Cu^0 to the Cu^I_2O (left) and Cu^I_2O to the $Cu^{II}O$ (right) drives the production of H_2O from H_2O_2 with C2 and C1, representing the energy differences at the two cathodes, respectively. Reprinted with permission from the Royal Society of Chemistry.

2.1.3. Metal-organic frameworks (MOFs)

Metal-organic frameworks are a type of nanomaterial that consists of metal ions or clusters of ions connected by organic linker groups. They are crystalline solids that are constructed by self-assembly of single metal cations or metal clusters with organic ligands that possess multiple binding sites [57,58]. Because of the specific shapes, MOFs are able to specifically and selectively recognize target substrates through Van Der Waals interactions of the framework surface with the substrate, metal-substrate interactions, and hydrogen bonding of the framework surface with the metal ion surface [59]. MOFs have been studied for their rich structural chemistry and potential applications, including biosensing. Their structure contains aromatic or conjugated π moieties (in a molecular system where p orbitals connect with delocalized electrons), which gives them enhanced optical properties [60]. In addition, the metal components also contribute to the increased MOF's optical properties, for example, lanthanide-based MOFs possess substantial photoluminescence (PL) potential [61]. MOFs are quite promising because of their structural diversity and their tunable chemical and physical properties. The unique chemistry structures have led to their function as effective glucose detectors [62,63]. They have also been used to detect other molecules such as thiamine and cysteine [64], as well as H_2O_2 or sulfhydryl-containing compounds. Two examples of the general catalytic mechanisms of MOFs are provided in Figure 5. For the most part, MOFs use functional pores to detect their substrates, which limits their application in biosensing because of the lack of available molecular recognition elements. To address this challenge, recognition capacity has been enhanced by adding open metal sites and specific sites on the pore surfaces, such as with the addition of the zirconium (Zr) ion site on MOFs that can promote the catalysis of H_2O_2 due to the high concentration of available Zr-OH catalytic sites [65].

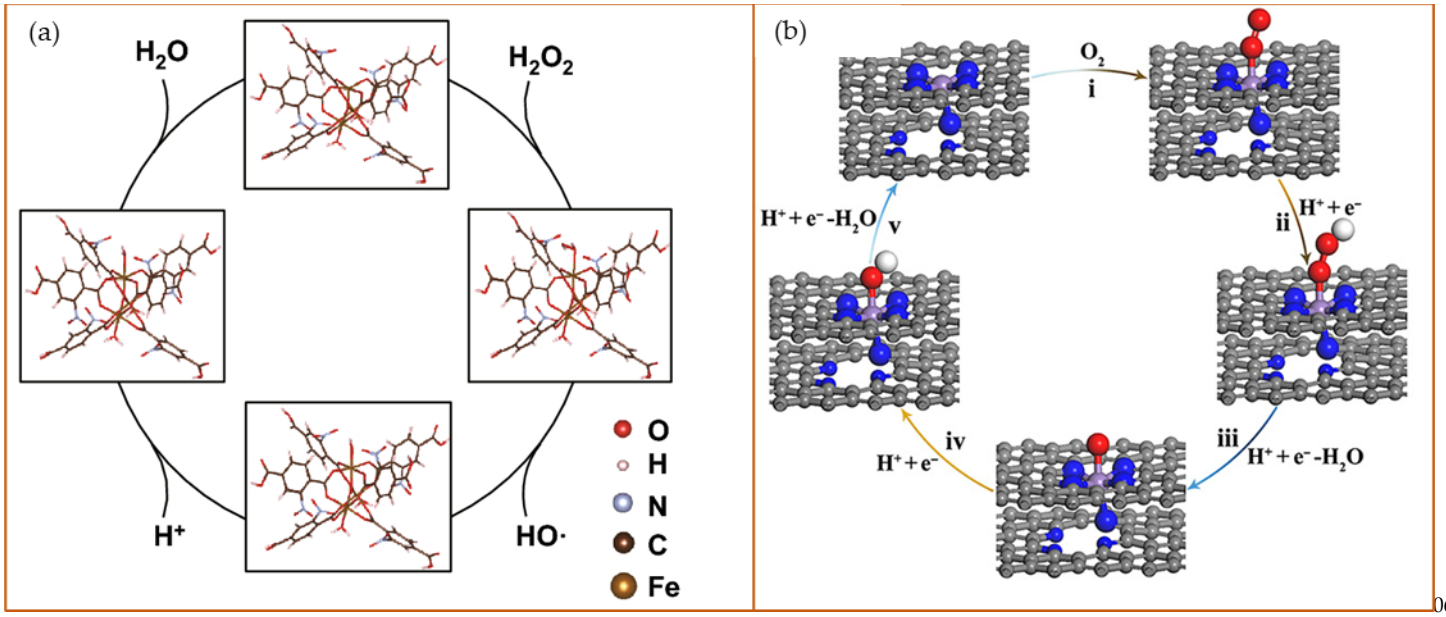

Figure 5. Examples of catalytic mechanism of MOFs. (a) Schematic diagram of peroxidase-like reaction of NO_2-MIL-101. in an acidic environment. In the MOFs, the Fe was employed at the reaction site to cleave H_2O_2 into an •OH and an hydroxyl group (-OH). The hrdrogen ions and -OH form the H_2O as a byproduct. Reprinted from [66]. Open access. (b) Schematic diagram of oxidase-like nanozyme: carbon nanoframe–confined axial N-coordinated single-atom Fe (FeN_5 SA/CNF). The pathways of O_2 reduction to H_2O is a four-electron process on the nanozyme surface: (i) $O_2 + H^+ + e^- = OOH$; (ii) $OOH + H^+ + e^- = O + H_2O$;(iii) $O + H^+ + e^- = OH$; (iv) $OH + H^+ + e^- = H_2O$. The color of the dots represent as follows: gray: C; blue: N; purple: Fe; red: O; white: H. Reprinted from [67]. Open access.

2.1.4. Carbon-based nanomaterials

Carbon-based nanomaterials (CNMs) generally have superoxide dismutase-like and peroxidase-like activities and include fullerenes, carbon nanotubes (CNTs), graphene, graphene quantum dots (GQDs), and carbon quantum dots (CQDs) [68,69]. They display excellent physical and chemical properties, high operational stability, and low cost compared with natural enzymes. The unique properties associated with CNMs rely on the fact that carbon is one of the few chemical elements with the ability to polymerize at the atomic level to form long carbon chains as the four electrons in the outer layer can form single, double, or triple bonds with other elements. Moreover, CNMs maintain robustness even

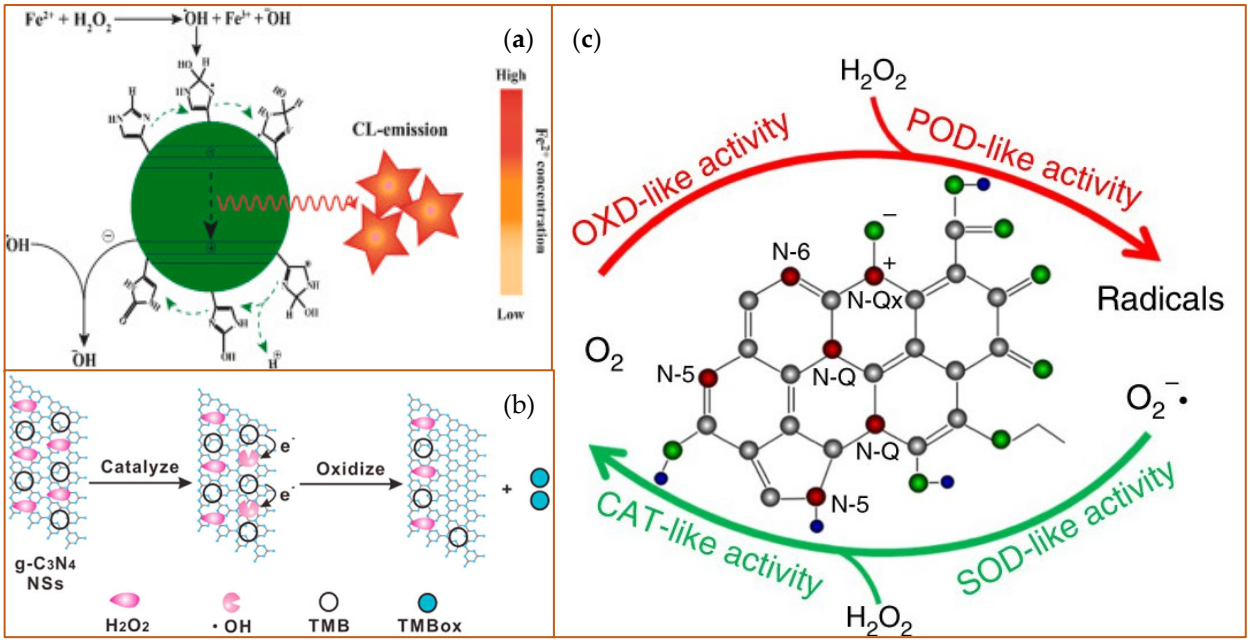

in stringent conditions, making them suitable for generating metal-free catalysts [70-72]. For example, carboxyl-modified graphene oxide (GO-COOH) has intrinsic peroxidase-like activity when catalyzing the reaction of the peroxidase substrate, TMB, in the presence of H_2O_2 to produce a blue colored reaction product [73]. A series of CNM-based biosensors for H_2O_2 [74,75] and other small molecules , ions [76,77], DNA [78,79], protein , and cancer cells have been developed, with the TMB used as a reaction substrate. The addition of TMB provides an added visual signal sensitivity since the TMB is readily oxidized by the carbon-based nanozyme. The general catalytic mechanisms of carbon-based nanozymes for detection of ions and small molecules and the applications based on the mechanisms are provided in Figure 6.

Figure 6. Schematic diagram of catalytic mechanisms of carbon based nanozymes. (a) Schematic illustration of the process of N-CDs enhanced Fenton system which was used for the sensitive and selective determination of Fe^{2+} ion (CL as chemiluminescence). Reprinted from [76], with permission from Elsevier. (b) Catalytic mechanism of the g-C_3N_4 nanosheets (NSs)-H_2O_2-TMB system. From left to right: H_2O_2 molecules interact with g-C_3N_4 NS to generate •OH and •OH oxidize TMB to form a blue product TMBox. Reprinted with permission from from [80] Copyright (2017) American Chemical Society. (c) Schematic dragram of enzyme-like activities of N-doped porous carbon nanospheres (N-PCNSs). N-PCNSs perform four enzyme-mimicing activities: oxidase (OXD), peroxidase (POD), catalase (CAT) and superoxide dismutase (SOD) for ROS regulation. Reprinted from [81]. Open access.

2.2. Nanozyme reaction mechanisms

Nanozymes were originally designed to overcome the limitations associated with large-scale, broad application of natural enzymes with the goal of maintaining a comparable catalytic mechanism relative to the specific substrates and in line with the desired outcome. Below is a summary of the general mechanisms utilized by nanozymes.

2.2.1. Peroxidase-like nanozymes

Peroxidase is an enzyme that catalyzes oxidation-reduction reactions using the mechanism of free radical transformation into oxidized or polymerized products [82]. Nanozymes in this group display similar mechanisms when catalyzing the subtrates (mostly H_2O_2), in which peroxides serve as electron donors. Research reported by Qu et al. has demonstrated that for carbon-based NPs, the functional groups "-C=O" and "-O=CO-" of GQDs can serve as catalytic activity sites and substrate-binding sites, respectively [83]. In contrast, the presence of an "-C-OH" group will inhibit the catalytic property of GQDs. At the mechanistic level, the aromatic domains of CNMs serve as the peroxidase mimic, catalyzing the reaction of H_2O_2 to ·OH whereas the -COOH reacts with H_2O_2 to generate -$C(OH)_2OOH$, and subsequent H_2O isolation produces -O=C-OOH [84]. In addition to the carbon-based nanozymes, metal oxidases such as Fe_3O_4 [4], single atom nanozymes such as Fe-N-C nanozymes [85], and MOFs such as Cu(PDA)(DMF) [86], also serve as peroxidase mimics to form ·OH when the substrate is H_2O_2 [4]. Knowing the mechanisms of peroxidase-like nanozymes benefits the design of the project for the catalysis of H_2O_2 and H_2O_2-based applications, including the biosensing of glucose [87], cysteine [88], and uric acid[89]. With the advancement of nanotechniques, researchers also used the peroxidase-like activity of nanomaterials for the detection of alkaline phosphatase [85], galactose [90], and ions [91]. In fact, efforts related to exploring the potential of peroxidase-like nanozymes not only focused on expanding the primary application but also on improving the catalytic properties of the nanozymes in order to decrease the impact coming from the reaction conditions. Qiaoshu Chen and coworkers designed negatively charged liposome-boosted, peroxidase-mimicking nanozymes to exhibit the activity in even alkaline conditions [92]. Liangjing Zhao and co-workers found that DNA modification made the activity 4.3-times higher compared with that of bare MoS_2 nanosheets [93] lending further support to the value of using peroxidase-like nanozymes.

2.2.2. Oxidase-like nanozymes

An oxidase is an enzyme that catalyzes oxidation-reduction reactions. In biological subjects, the oxidases could be used to catalyze the production of glucose , monoamine [94], and other substrates [95,96]. The oxidase-like nanozymes are designed to mimic the properties of oxidases. The oxidase-like nanozymes can be separated into two groups based largely on their catalytic mechanism: the glucose oxidase-like group and the sulfite oxidase-like group. Noble metals such as Au are able to form Au^{+}-O_2^{-} or Au^{2+}-O_2^{2-} couples, generating a dioxo-Au intermediate that can serve as a bridge to transfer electrons from glucose and H_2O_2 to dioxygen and water in a glucose detection reaction [97]. An alternative mechanism is mediated by the sulfite oxidase-like group in which the sulfite oxidase functions as the electron acceptor during catalysis. For example, molybdenum trioxide (MoO_3) NPs possess an intrinsic sulfite oxidase-like activity the mechanism of which has been determined: MoO_3 NPs catalyze the oxidation of colorless 2,2′-azino-bis (3-ethylbenzothiazoline-6-sulfonic acid) (ABTS) to generate a green reaction product. The mechanism was used to detect acid phosphatase (ACP) because the ACP catalyzed the hydrolysis of the ascorbic acid 2-phosphate (AAP) substrate to produce ascorbic acid (AA). As a result, the AA reduces the colorimetric output from ABTS oxidation [98] generating a highly sensitive biosensing tool.

2.2.3. Superoxide dismutase-like nanoparticles

Ceria (CeO_2) NPs are the main members of superoxide dismutase-like nanoparticles. Because of the oxidase states of Ce^{3+} and Ce^{4+}, nanoceria may transition between the two in a redox reaction, producing oxygen vacancy sites. Based on the redox capacity, nanoceria is concered an acceptable oxygen buffer [99,100]. This unique electron structure makes CeO_2 a quite essential example of a superoxide dismutase-like nanoparticle [101]. The main catalysis process is illustrated in Figure 7.

Overall, nanozymes function as peroxidase, oxidase, superoxide dismutase or other enzymes based on the characteristics and potential of their active components, including the different charge status or the inate properties derived from their structures. Different nanomaterials mimic the activity of different enzymes. The mimic activity can be affected by the structure of nanozymes, including the particle size [102], surface modification [103,104], and morphology [105] to improve the catalytic activity, substrate specificity, and stability [106,107]. Many nanozymes are size-dependent since smaller nanozymes show a higher surface-to-volume ratio, which enhances the interactions with substrates because of the more active sites exposed [102]. But sometimes larger nanozymes may show higher activity, possibly due to the fact that there are more metal ions [108], the presence of suitable valences [109], or the existence of redox reaction potential [110]. Excellent examples of these include two dimensional (2D) nanomaterials, with the characteristic single-layer nanosheet structure that can include graphene, hexagonal boron nitride, transition metal dichalcogenides, graphitic carbon nitride, layered metal oxides or layered double hydroxides. The advantage of these 2D nanomaterials is that they prossess high specific surface area, numerous active sites, the ability to act as supporting materials within a larger structure, and show enhanced nanozyme catalysis activity [111-114]. There is also tremendous potential for surface modification which can include coating with small molecules, ions, and polymers on the surface, thereby increasing the stability and active reaction sites available. These surface modifications, therefore, can be used to adjust or "fine-tune" the catalysis properties of this class of nanozymes [115-117]. Additionally, the morphology and crystallographic planes have important effects on modulating the catalytic activity because the different amounts of types of available bond structures and various arrangements of atoms in the nanozymes determines the selectivity and reactivity of nanozyme, overall [118,119]. In addition to the structural composition [120] of nanozymes, their reaction environment, such as pH, temperature, light, etc, are key factors that can affect nanozyme activity [121-123]. Determining the relationship between the structure and the catalysis activity will help us to design nanozymes in the future with high activity and

specificity. With the development of nanotechnology, more nanozymes will be designed and studied to further advancements in biosensing and related fields.

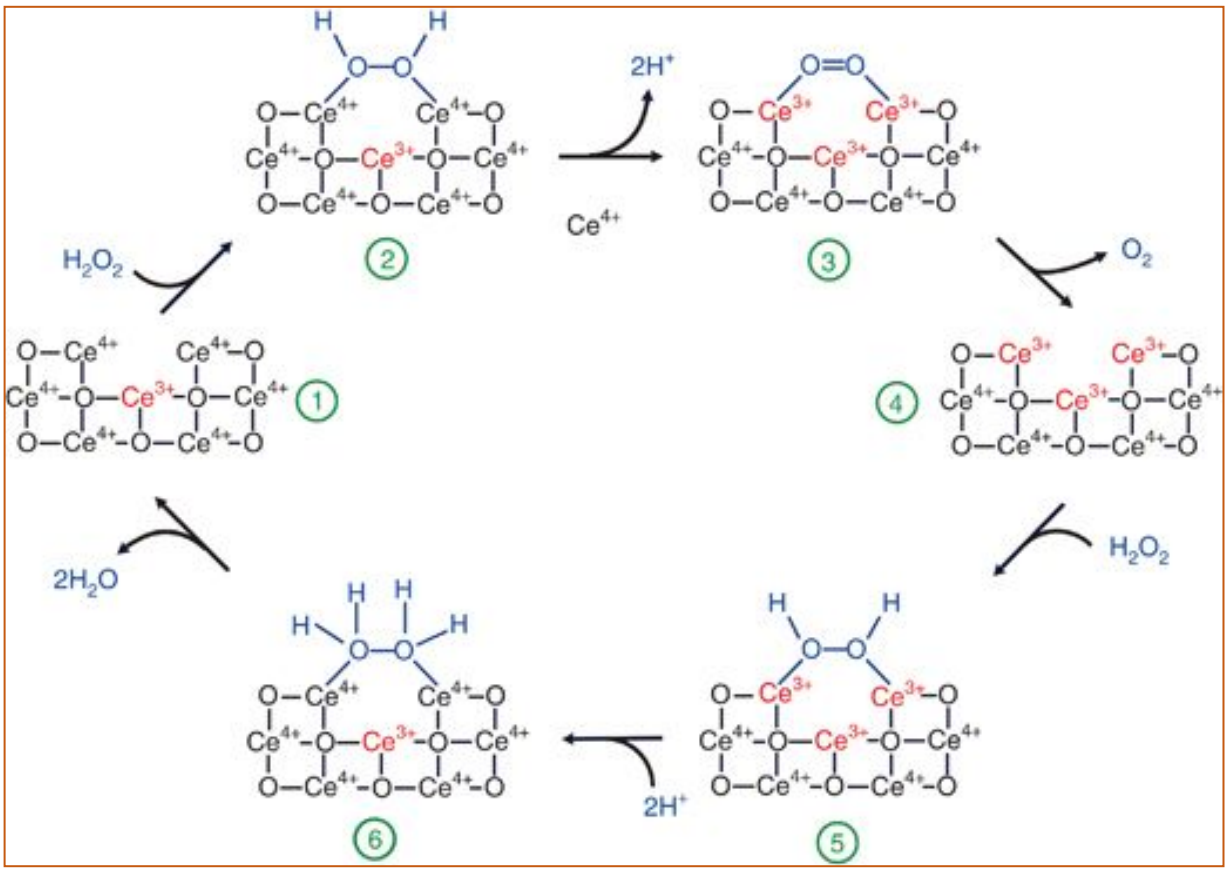

Figure 7. A review of the reaction mechanism of cerium oxide nanoparticles (CeO NP) catalyzes the H_2O_2 with its superoxide dismutase-like activity. During the entire process, the amount of bound Ce^{3+}/Ce^{4+} (red font) changes with the structure of the oxygen containing groups (blue font), causing the catalyzation of H_2O_2 [100]. The reactants and products are indicated at each stage of the reaction, 1-6. Reprinted from [100],with the permission from Nanoscale.

3. Nanozymes and their potential applications in biosensing

With the rapid technical advances associated with nanozymes, the broad application of nanozymes extended apace to different fields, including environmental protection [36], anti-bacterial treatment [124], cancer therapy [125], cyto-protection [126], biosensing [104], and more [127]. Advances were achieved using different methodological approaches, including optical (fluorescent [128] and photoluminescent [129]) and electrochemical (voltametric [130] and amperometric [131]) detection strategies. Among these applications, the usage of nanozymes in biosensing has drawn notable attention because of the increased need for stable, cost-effective catalytic tools for use in clinical and basic research. While the classical view of biosensors generally refers to a biological component in combination with a chemical component or partner, we take a more broad view herein to include chemical structures (and/or devices) that can be used to detect a biologically-relevant target. The most rapidly expanding area of research and application is in biosensing with the major application approaches highlighted below.

3.1.Detection of ions

Metal ions, especially heavy metals, are not easily metabolized and, therefore, accumulate in organs resulting in tissue damage and increasing disease vulnerability over time [132,133]. As a result, the accurate detection of metal ions in the environment or in tissues

is urgently needed as a prelude to environmental remediation [134] or clinical intervention strategies [29,135]. Here we give two examples linked to mercury (Hg) and Cu ions to illustrate the critical characteristics of the materials and the proposed mechanism of action for target ion detection.

As an extremely toxic metal, mercury is one of the important targets detected by different nanozymes . Mercury exposure has been linked to brain, kidney, and lung damage and has been identified as a primary cause or contributing factor in several diseases, including Minamata disease , Alzheimer's disease , cardiovascular disease [136] among many. Cao and his colleagues found that when Au NPs were functionalized with oligoethylene glycol (OEG), the formation of an Au-Hg amalgamation was enhanced. Indeed, with this approach, they were able to achieve a low limit of detection (10 ppb) in lab-based water samples (Figure 8a) [137]. Platinum (Pt) nanozymes, based on their peroxidase-like function, can also be used to detect mercury ions, because Hg^{2+} was specifically shown to inhibit the catalytic properties of the nanozymes in a luminol system. Zhao and coworkers found that Pt NPs can catalyze the chemiluminescence (CL) of the luminol system. They took advantage of this catalysis mechanism and applied it toward Hg^{2+} detection, as the Hg^{2+} could further enhance the CL intensity in the Pt NPs-luminol CL system. With this approach, they were able to detect Hg^{2+} and achieved a low-end detection limit of 8.6 nM compared with other methods (LOD ranges from 3.3 nM to 338 nM) (Figure 8b) [138]. Based on the intrinsic properties of Au and Pt, Wang and colleagues designed a Au@AgPt NP with surface-enhanced Raman scattering (SERS) -active peroxidase-like activity which could be used to detect the signal molecules (which generate SERS or colorimetric signal) [139]. SERS is a sensing technique in which inelastic light scattering by molecules is enhanced when the molecules are adsorbed onto corrugated metal surfaces [140]). With the help of a colorimetric/SERS dual-mode probe integrated with the advantages of facile detection by colorimetric analysis and a high-sensitivity trace assay by SERS, Au@AgPt NPs achieved the limit of detections (LODs) of colorimetric analysis of 0.52 μM and by SERS assay of 0.28 nM. Besides the noble metal examples provided, metal oxides nanomaterials can also be used to detect Hg^{2+} [141].

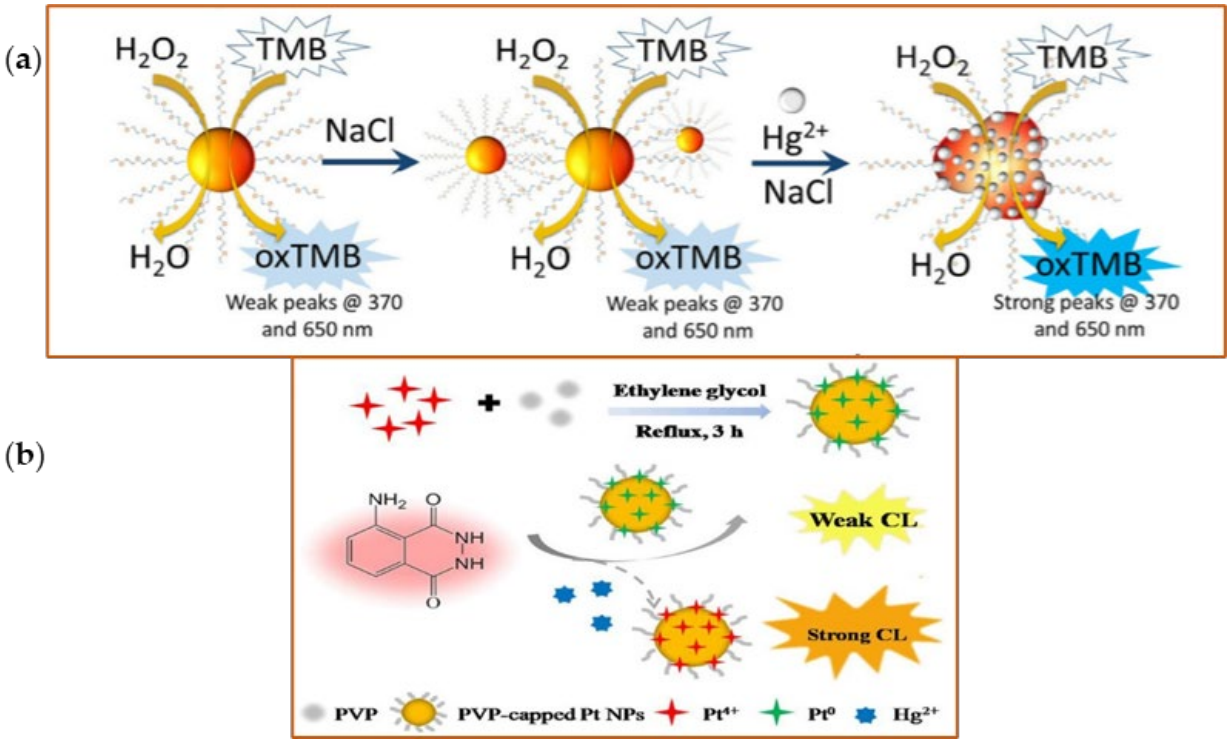

Figure 8. Schematic illustration of detection of Hg^{2+} with different nanozymes. (a) Schematic illustration of the detection of Hg^{2+} of Au NPs. Left side, Au NPs shows stability in high electrolyte solutions. Right side, in the presence of Hg^{2+}, the catalytic activity of the Au NPs was improved, with strong fluorescence signal detected at the indicated wavelengths [137]. Open access.

(b) Schematic illustration of Hg^{2+} detection by Pt NPs. Pt NPs capped with PVP (polyvinyl pyrrolidone) were synthesized in the mixture solution of Pt^{4+}, PVP and ethylene glycol under 3 hours reflux. With the peroxidase-like activity, PVP-capped Pt NPs ctatlyzed the CL of the luminol system in the presence of Hg^{2+}. Reprint from [138], with permission from John Wiley and Sons.

Copper (Cu) is an important element for biological organisms and the proteins that contain Cu are critical for a variety of physiological processes [142,143]. However, high concentrations of Cu can cause cellular damage as has been demonstrated in Wilson's disease, an inherited disorder characterized by abnormal accumulation of Cu, predominantly in the liver [144]. Therefore, it is important to perform Cu ion detection with the lowest LOD possible. In order to address this challenge, a wide range of materials have been used to synthesize nanozymes optimal for sensitive Cu detection. Wang and coworkers reported a rapid and sensitive fluorescence nitrogen-doped GQDs (N-GQDs), which were utilized as sensing probes for the selective detection of Cu^{2+} by taking advantage of the PL quenching of N-GQDs after adding Cu^{2+} [145]. The detection limit for Cu^{2+} was found to be 57 nM. Yan Liu and coworkers designed nanozymes with noble elements; Au nanoclusters designed for the detection of Cu^{2+} in blood samples attained a minimum detection limit of 0.1 nM. This lower LOD was achieved by the combination of peroxidase-like nanozyme activity of the Au cluster with the amino acids' ambidentate of histidine (His) because the peroxidase-like activity of histidine-Au nanocluster (His-AuNCs) could be decreased by adding Cu ions. Additional methods to detect Cu^{2+} have been developed. Raibaut designed a nanozyme that combined the selectivity and suitable affinity of the amino-terminal Cu^{2+}- and Ni^{2+}- binding (ATCUN, also called Xxx-Zzz-His peptide motif, Xxx can be any amino acid, Zzz can be any but not proline) with the long-lifetime emission of the lanthanide Tb^{3+} to achieve the selective and reversible detection of Cu^{2+} [146]. These examples highlight the value of using nanozymes to detect Cu ions and similar design approaches can be applied to other biosensing targets.

3.2. Detection of small molecules

Hydrogen peroxide (H_2O_2), an essential oxidizing agent, is generated during many physiological processes, including the oxidation of glucose, and is harmful to cells because of the high oxidation activity relative to proteins and DNA. The detection of H_2O_2 could help clinicians and researchers investigate disease progression and mechanisms, such as detecting early stage vascular disease [147]. Therefore, different methods have been developed to detect H_2O_2 using different nanozymes with a wide range of intrinsic catalytic properties [148]. Since H_2O_2 is an oxidation product of glucose in the presence of glucose oxidase, there is a clear link between these critical molecules. In fact, clinical and basic research approaches will often attempt to detect H_2O_2 and glucose in parallel using compatible approaches [149]. Liang and coworkers designed Vanadium oxide (V_2O_5)-based nanozymes to detect H_2O_2 and glucose because of their peroxidase-like activity in the presence of the enzyme substrate o-phenylenediamine (OPD) [18]. With this dual approach, (V_2O_5)-based nanozymes were able to achieve a minimum detection limit of 1 μM for H_2O_2 and 10 μM for glucose. The detection of H_2O_2 is conducted by various nanozymes, not limited to metal oxides nanozymes. Noble metal nanoparticles could be used to detect H_2O_2 and glucose as well. Wang and coworkers designed palladium-based nanostructures, PdCuAu NPs, which have excellent catalytic performance as peroxidase-like enzymes [150]. The combination of PdCuAu NPs can catalyze TMB rapidly in the presence of H_2O_2 and oxidize it to visible blue products (oxTMB). The LOD were 5 nM and 25 nM for H_2O_2 and glucose, respectively. As to be expected, some MOFs were designed to detect the critical molecules H_2O_2 and glucose. In Yuan's work, Fe-MOFs, using the ferric ion as the metal center, incorporated a porphyrin analog as the organic ligand to work as a metalloenzyme which displays unique catalytic properties. This analytical tool was developed to detect H_2O_2 and glucose based on its high peroxidase-like catalytic activity [151]. The detection limits of H_2O_2 and glucose were 1.2 μM and 0.6 μM, respectively, using this approach.

There are other small molecules that have been detected successfully using nanozymes as biosensors. Sharma and coworkers designed a nanozyme that combined Au nanoparticle (GNPs) with an ssDNA aptamer (Ky2), that shows specific molecular recognition elements for kanamycin and blocked the ability of GNPs to catalyze when bound to the Ky2 aptamer. However, in the presence of kanamycin, the Ky2 transferred to the kanamycin and the GNPs were able to catalyze the colorimetric detection of TMB, generating an on/off switch mechanism that was remarkably effective [21]. M. Shamsipur and coworkers synthesized a new colorimetric biosensor for glutathione (GSH) based on its radical restoration ability. The carbon nanodots (CDs), enhance the free radical formation generated by the oxidation of TMB by CDs. The free radical cation concentration was related to the GSH concentration, permitting indirect calculation of GSH concentration with a low LOD: 0.3 μM [152]. With new nanozyme synthesis and design techniques developing at a rapid rate, the ability to detect different molecular targets with greater sensitivity and accuracy is increasing. The investigation of potential biosensing applications and the promising potential of nanozymes is attracting increasing research and clinical attention worldwide.

3.3. Detection of nucleic acids

The detection of nucleic acids by biosensors has been successful using a variety of strategies and engineered for different applications. For DNA, nanozymes are not just used to detect double-stranded DNA, but also single-strand DNA, mutant DNA (compared to "normal" sequence), as well as DNA modifications, such as methylation. Shen and colleagues designed a DNA-controlled strategy for the growth of Pt NPs on graphene oxide (GO–PtNPs) to detect specific DNA targets [153]. They used two hairpin ssDNA and one triplex-hybridization chain reaction (tHCR) to trigger hybridization with a DNA target to form a long double-stranded DNA structure. This allowed the Pt NPs to grow with the Pt precursor on the surface of GO and generate the TMB-based colorimetric assay reactant. However if there is no DNA target, then the two short hairpin ssDNA would attach on the surface of GO, and Pt NPs growth on the surface of ssDNA occurred without the colorimetric reaction. The proposed method showed very high sensitivity with the detection limits down to 14.6 pM for mutant Kirsten RAt Sarcoma (KRAS) DNA and 21.7 pM for let-7a microRNA, both of which are frequently mutated in tumors. Yao and coworkers designed TiO_2 nanowires (NWs) as an effective sensing platform for rapid fluorescence detection of single- and double-stranded DNA [154]. The fluorescence labeled DNA probes were effectively absorbed by TiO_2 NWs, and the leading fluorescence intensity helps with the detection of DNA. Zheng and coworkers proposed unmodified Au NPs for rapid colorimetric detection of DNA methylation based on the difference in electrostatic attraction of single-stranded DNA and double-stranded DNA against salt-induced aggregation of Au NPs. The principle is that the methylated P53 fragment maintains the methylation status after the bisulfite treatment and leads to proper match with a designed ssDNA and subsequent aggregation with the AuNPs. An unmethylated P53 fragment will lead to a mismatch with designed ssDNA and dispersion under the treatment of AuNPs. This method has demonstrated a DNA methylated detection limit of 8.47 nM [79] and highlights this approach as a potential strategy to investigate epigenetic modifications of the chromatin landscape.

For RNA detection, identifying specific miRNAs associated with the disease are particularly important in cancer detection and staging. For example, miR-21, a potential biomarker of oral cancer [155], ovarian cancer [156], and other cancers can now be detected using nanozyme biosensors. An ultrasensitive electrochemical biosensor for miR-21 detection was designed on the basis of a padlock exponential rolling circle amplification (P-ERCA) assay [157] and $CoFe_2O_4$ magnetic nanoparticles ($CoFe_2O_4$ MNPs) [158]. This assay is a highly specific and sensitive amplification method with a detection limit down to the zeptomole level designed with a padlock probe composed of a hybridization sequence to miRNA and a nicking target site for the endonuclease. With this approach, Nan Yu and

colleagues achieved a wide dynamic range of 1 fM to 2 nM with a low detection limit of 0.3 fM for miR-21 detection [158]. Also, miRNA-155, an oncogenic miRNA in breast cancer [159], non-small cell lung cancer [160], and other cancers, is detectable using a biosensor combined with a nanoscale copper-based metal-organic framework assembled by Pt NPs and horseradish peroxidase (Cu-NMOF@PtNPs/HRP) and a toehold strand displacement reaction (TSDR, a enzyme-free DNA strand displacement reaction based on the principle of toehold exchange to achieve the DNA amplification [161]) to improve the multiple amplifications [162]. In the presence of miRNA-155, the TSDR system would be triggered, leading to hybridization of the nanoprobe. With this approach, a minimal detection limit of 0.13 fM miRNA-155 can be achieved in RNA extracts of serum and MCF-7 and MDA-MB-231 cell lysates [99]. As the need for rapid and early detection of cancer biomarkers increases, the nanozyme-based biosensors with the highest sensitivity will be of tremendous value.

3.4. Detection of proteins

Proteins play essential roles in our body and misregulation or misexpression of proteins is often at the heart of a variety of diseases. As a result, changes in protein expression, post-translational modification, or folding can be used as biomarkers or hallmarks of disease or disease stage. Therefore, developing approaches that allow for improved quality and quantity of detection is important for the diagnosis and treatment of diseases. Several nanozyme-based approaches have been designed expressly for the purpose of ultrasensitive biomarker detection. Wang and colleagues designed Au/Co bimetallic nanoparticles decorating a hollow nanopore carbon framework (Au/Co@HNCF) for the detection of uric acid in human serum with the limit of detection at 0.023 μM [163]. Uric acid is a hallmark of gout , tumor lysis syndrome , Type 2 diabetes , and other health problems. MOFs, as promising nanoparticles, may have more potential applications compared to metric nanoparticles based on their structure, potential for surface modifications, and tunability. Fengting Li and coworkers used Fe-MIL-88A, a photoactive ion-based MOF material , to detect thrombin based on the peroxidase-like catalytic activity of Fe-MIL-88A towards TMB [164]. Thrombin is an important serine protease, catalyzing many coagulation-related processes, such as cerebral ischemia and infarction [165]. In the presence of thrombin and its corresponding aptamer, the mimetic activity of Fe-MIL-88A is strongly inhibited and is the basis for colorimetric detection and quantification of thrombin with a low LOD of 10 nM. The advantage of this method is that the thrombin could be changed to other target proteins when applying the corresponding aptamers. An easy and simple method for synthesiszing nanozymes and detecting various proteins is advantageous for clinic diagnosis and other fields. Detection of various proteins with nanozymes is a large-scale project with several potential strategies and merits future research focus.

3.5. Cancer cell detection

The detection of cancer cells in the human body is a promising field for biosensors, as the selectivity and sensitivity of the methods are relevant to clinical diagnosis, treatment and prognosis of cancers. Tian and coworker designed CuO nanozymes as a catalyst for the detection of circulating tumor cells with the support materials of reduced graphene oxide/gold nanoparticles composites (rGO/Au NPs composites). On the rGO/Au NPs composites, the MUC-1 (Mucin 1, a cell surface associated protein) aptamer was used to recognize the MCF-7 cells because of the over-expression MUC-1 on the surface. The CuO nanozyme is used as a signal-amplifying nanoprobe and achieves a low detection limit of 27 cells per mL^{-1} [54]. Zhao and coworkers designed a cancer cell detection method that combines Au, whole tobacco mosaic virus (TMV), and folic acid in order to target folic acid receptors on the surface of HeLa cells and other tumor cells [166]. The authors developed an Au@TMV nanowire (AT) conjugated folic acids (FA) complex (ATF) [166]. Because folate receptors are overexpressed on the surface of Hela and other tumor cells, their receptors could bind to the folic acid in the complex. Subsequently, the peroxidase properties of ATF were used to convey a TMB/H_2O_2-based colorimetric method to detect folic-

acid expressing cancer cells in a mixed population with a detection limit of 2000 cancer cells/mL could be achieved, which is higher than the other nanoparticles using TMV as the basic material [167,168]. While Au NPs can be used for the detection of cancer cells, there are active areas of research investigating other potential sources for materials, focusing on increased specificity and reduced toxicity. Tuncel and colleagues have developed a rapid colorimetric method to detect tumor cells that utilizes an externalizable complex of monodisperse-porous silica microsphere that contains immobilized Fe_3O_4 NPs (Fe_3O_4@SiO_2 microspheres). After combination with hyaluronic acid (HA), a ligand sensitive to CD44 receptors on tumor cells, the nanocomposites could be taken up by human cervical cancer (HeLa) cells and primary brain tumor cells T98 G cells via pinocytosis, with the cell detection achieved by oxidation of TMB generated by the catalytic properties of the Fe_3O_4@SiO_2 microspheres [169]. The detection of cancer cells is achieved by the evaluation of the over-expressed surface biomarkers (eg, CD44 receptors, folic acid [170]) or the amount of internalization of nanozymes that caused changes in cancer cells. There are more methods under evaluation.

Table 1. Nanozyme classification, major subtrates and detection methods

Groups	Nanozymes	Targets	Signal	Detection methods	Ref.
Metal-based nanozymes	Au@Pt nanozyme	Ag^+	extinction spectra	UV–visible spectroscopy	[36]
	Au NPs	H_2O_2	absorbance	adsorption spectroscopy	[31]
	Au NPs	microRNA	surface plasmon resonance (SPR)	hEC-SPR1010 device	[34]
	Au NPs	cancer cells	absorbance	adsorption spectroscopy	[35]
Metal oxidase-based nanozymes	Fe_2O_3 NPs	exosomes	absorbance	adsorption spectroscopy	[41]
	CeO2 microspheres	phosphoprotein	absorbance	UV–Vis spectrophotometer	[101]
	Fe_3O_4@SiO_2 microspheres	cancer cells	absorbance	UV–vis spectrophoto	[169]
	hollow MnFeO oxide	Hg^{2+}	absorbance	UV–vis spectrophotometer	[141]
	MnO_2 NPs	H_2O_2	fluorescence	confocal laser scanning microscopy	[53]
MOFs	Ni/Cu-MOFs	glucose	current	semiconductor parameter analyzer and four-point probe station	[62]
	Cu-NMOF@PtNPs/HRP	miR-155	square wave voltammetry	electrochemical workstation	[162]
	Ni-hemin MOFs	cancer cells	absorbance	SPECTROD 250-analytikjena spectrophotometer	[170]
Carbon-based nanozymes	N-CDs	Fe^{2+}	chemiluminescence	BPCL Luminescence Analyzer	[76]
	C-dots	DNA damage	fluorescence	an Infinite 200 PRO multimode reader	[78]
	GO based nanozyme	homocysteine	absorbance	UV-vis spectrophotometer	[115]
	rGO/Au NPs composites	cancer cells	amperometric signals	CHI660E electrochemical workstation	[54]

4. Challenges and future directions for nanozyme research

Although nanozymes show excellent advantages over the traditional biocatalyst approach, there are several challenges that remain to be overcome. One of the major challenges is the poor selectivity and lower sensitivity of nanozymes compared with natural enzymes. The second challenge lies in the fact that there are a far greater number of enzymes than there are currently available nanozyme mimics. If we could develop general nanozyme design workflows along with increasing the number of nanozymes designed

to mimic physiologically and clinically relevant enzymes, the potential applications would be essentially unlimited. The third major challenge is related to toxicity concerns because few of the mechanisms or potential toxicities have been identified to date. This latter challenge will likely remain a major hurdle to overcome in the field of nanozyme application in biosensing and will undoubtedly be an active area of future research.

Based on these challenges, more investigation is imperative to improve the catalytic activity and specificity for nanozymes, while reducing potential toxicity. With the rapid development of nanotechnology, more nanomaterials are currently being developed for use as biosensors due to their enzyme-like properties and ability to mimic catalase, oxidase, peroxidase, phosphatase, and superoxidase dismutase activity. The catalytic activity is determined by the intrinsic chemical structure. Because of the low sensitivity and selectivity, as well as the catalytic property of nanozymes compared with enzymes, studies focused on improving the catalytic activity have drawn the most attention. For example, nanoparticles capped with DNA have been found to improve the oxidation reaction rate because of the long length and sequence [171]. Liu and coworkers found that the iron oxide nanoparticles capped with DNA demonstrated higher peroxidase activity than naked nanoparticles. The catalysis activity was enhanced with longer DNA strands and a higher proportion of cytosine relative to the other nucleotides [171]. Lin and coworker used Tris-(benzyltriazolylmethyl) amine (TBTA) to improve the sensitivity and stability of the sensing system to achieve a sensitive detection of Cu [172].

Another research area ripe for exploration is the expansion of type and range of nanozyme targets. For example, the detection of tumor markers could be designed to improve both the diagnosis accuracy and time-to-diagnosis, particularly in point of care treatment [173,174]. If diagnosing tumor can be done earlier, and more accurately, the treatment efficacy would be dramatically improved. Additionally, the mechanism of inhibition on the enzymatic activities of nanozymes is an important focus area. Further, in their recent review, Fan and colleagues highlight the importance of research on the factors which impact the catalytic efficiency and detection limits of nanozymes [175]. There is also considerable opportunity at the level of the properties and potential of nanomaterials, themselves, to explore functional mimics that can be utilized to expand biosensing targets.

Rational design of nanomaterials means "design-for-purpose", a strategy of designing new nanomaterials based on the ability to predict how the new nanomaterial can affect the target and exhibit the appropriate catalytic function to match the target strategy [176]. The clear insights resulting from integration of active sites, knowledge of nanozyme mechanisms, the grasp of new nanomatierials, and the ability to fuse these together will help researchers to design a new cadre of nanozymes with high performance potential [177]. The rational design of nanozymes is of great significance for biosensing, biomedical application, and other fields [178-180]. For example, Qian Wang and co-workers designed a N-doped carbon nanocage with Co-Nx active sites (CoNx-NC), as one of the metal nitrogen-doped carbon (metal-NC) catalysts [181]. This unique nanozyme shows both catalase- and oxidase- like properties to detect acethlcholinesterase without peroxidase-like properties. CoNx-NC decomposed H_2O_2 into O_2, thus oxidizing TMB into a blue reaction product. Based on the inhibitory effect of thiocholine on the TMB color reaction, the thiocholine is produced in the presence of acethlcholinesterase, which can be used as an indicator of Alzheimer's disease. Yan Liu and coworkers designed an arginine (R)-rich peptide/platinum hybrid colloid nanoparticle cluster to mimic the uricase/catalase system and superoxide diemutase/catalase system to degrade uric acid and eliminate ROS [184]. This approach has potential applications for detecting gout and for use in hyperuricemia therapy [182]. To achieve the defined goal, all the characterization and components of nanozymes need to be designed to serve the specific functions and then investigated thoroughly for efficacy. For example, in the CoNx-NC project, to achieve the detection of acethlcholinesterase, the Co-Co Prussian blue analogues, classic cubic MOFs were used as precursors, while polyvinylpyrrolidone (PVP) was introduced to provide extra nitrogen for doping to support formation and inhibit aggregation. After pyrolysis and acid etching,

the Co-Nx-NC was synthesized and applied for acetylcholinesterase detection with oxidase- and catalase- mimicking properties of Co-Nx-NC. Another example is biomimetic nanozymes for glucose detection that have been designed by Rui Geng and coworkers [183]. They combined amphiphilic amino acid, a histine derivative for fabricating nanoassemblies with the assistance of metal ions, and a heme derivative, which included iron ions in the center. The side chain of histine derivative and the iron ion of heme devivative combined through noncovalent interactions and showed peroxidase mimicking property. In this way, supramolecular peptide nanozymes with peroxidase-like activity were designed and synthesized for glucose sensing.

Collectively, nanozyme research and nanozyme applications in biosensing represent tremendous potential for clinical and research benefit. With increasing focus on designing nanozymes with increased specificity and reduced toxicity there is promise that we can hit a broad range of biosensing targets.

Author Contributions: Y.W. prepared the draft and all co-authors contributed to conceptual discussions, writing, and editing. All authors have read and agreed to the published version of the manuscript.

Funding: This work was partially supported by the National Science Foundation grant CHE 1709160 and Cooperative Agreement Award OIA #1946202 (JXZ), the University of North Dakota Program for "Applied Research to Address the State's Critical Needs Initiative" (JXZ), and the National Institutes of Health Award COBRE grant (2P20GM104360-06A1; DCD, Project Director; R. Vaughan, PI).

Acknowledgments: The authors thank Dr. Xu Steven Wu (Department of Chemistry, University of South Dakota) for his initial discussion contributions to the idea for this review and Dr. Alena Kubatova (Department of Chemistry, UND) for her thoughtful comments at the early stages of this work. The authors also thank Ms. Chloe Kaelberer and Ms. Elisabeth Kolb for their editorial feedback at the final stages of this project.

Conflicts of Interest: The authors declare no conflict of interest.

Abbreviations

The following abbreviations are used in this manuscript:

ROS: reactive oxygen species; 5mC: methylated cytosine; AA: ascorbic acid; AAP: ascorbic acid 2-phosphate; ABTS:2,2′-azino-bis(3-ethylbenzothiazoline-6-sulfonic acid)； ACP: acid phosphatase; AFP: alpha fetoprotein; AOPs: advanced oxidation processes; AT: Au@TMV nanowire; ATBTS: colorless 2,2′-azino-bis (3-ethylbenzothiazoline-6-sulfonic acid); ATCUN: amino terminal Cu2+- and Ni2+-binding; ATF: an Au@TMV nanowire (AT) conjugated folic acids (FA) complex ; Au NPs: gold nanoparticles; BMCNTs: bamboo-like magnetic carbon nanotubes; BQ: benzoquinone; CeONP: cerium oxide nanoparticle; C-IONPs: carboxyl group-functionalized iron oxide nanoparticles; CL: chemiluminescence; CNMs: Carbon-based nanomaterials; CNTs: carbon nanotubes; CQDs: carbon quantum dots; CuSPE: copper-plated screen-printed carbon electrode; EDTA: Ethylenediaminetetraacetic acid; EtBr: ethidium bromide; Exo: exosomes; FA: folic acids; FAM: fluorophore; FIA: low injection analysis; FRET: Förster resonance energy transfer; GFA: folic acid graphene oxide-Au nanocluster hybrid; GO-COOH: Carboxyl-modified graphene oxide ; GOx: glucose oxidase; GQDs: graphene quantum dots; H_2O_2: Hydrogen peroxide; HA: hyaluronic acid; HCR: hybridization chain reaction; HQ: hydroquinone; KRAS: Kirsten Rat Sarcoma; LOD: the limit of detection; MCC: $Mn_3[Co(CN)_6]_2$; Me-TTFTB : tetrathiafulvalene tetramethylbenzoate; MIL: Matériaux Institut Lavoisier; miRNA: microRNA; MOFs: Metal-organic frameworks; MUC 1: Mucin 1; N-CDs: N-doped carbon dots; N-GQDs: nitrogen-doped graphene quantum dots; NWs: nanowires; OEG: oligo-ethylene glycol; OPD: o-phenylenediamine; PL: photoluminescence; POMs: Polyoxometalates; Pt-NPs: platinum nanoparticles; PVP: poly-vinylpyrrolidone; RhB: Rhodamine B; SERS: surface-enhanced Raman scattering; SPCEs: screen-printed carbon electrodes; SPR: surface plasmon resonance; ssDNA: single-stranded DNA; T: thymine; TBTA: Tris-(benzyltriazolylmethyl) amine; tHCR: triplex-hybridization chain reaction; TMB: 3,3,5,5-tetramethylbenzidine; TMV: tobacco mosaic virus; TSDR: toehold strand displacement reaction; TTFTB: tetrathiafulvalene tetrabenzoate

References

1. Jaeger, K.-E.; Eggert, T. Enantioselective biocatalysis optimized by directed evolution. *Curr Opin Biotechnol* **2004**, *15*, 305-313, doi:10.1016/j.copbio.2004.06.007.
2. Wu, S.; Tatarchuk, B.J.; Adamczyk, A.J. Ethylene oxidation on unpromoted silver catalysts: Reaction pathway and selectivity analysis using DFT calculations. *Surface Science* **2021**, *708*, 121834, doi:10.1016/j.susc.2021.121834.
3. Zhou, Y.; Liu, B.; Yang, R.; Liu, J. Filling in the Gaps between Nanozymes and Enzymes: Challenges and Opportunities. *Bioconjugate Chemistry* **2017**, *28*, 2903-2909, doi:10.1021/acs.bioconjchem.7b00673.
4. Wang, Q.; Zhang, X.; Huang, L.; Zhang, Z.; Dong, S. One-Pot Synthesis of Fe3O4 Nanoparticle Loaded 3D Porous Graphene Nanocomposites with Enhanced Nanozyme Activity for Glucose Detection. *ACS Appl Mater Interfaces* **2017**, *9*, 7465-7471, doi:10.1021/acsami.6b16034.
5. Han, L.; Li, C.; Zhang, T.; Lang, Q.; Liu, A. Au@Ag Heterogeneous Nanorods as Nanozyme Interfaces with Peroxidase-Like Activity and Their Application for One-Pot Analysis of Glucose at Nearly Neutral pH. *ACS Appl Mater Interfaces* **2015**, *7*, 14463-14470, doi:10.1021/acsami.5b03591.
6. Jin, R.; Zeng, C.; Zhou, M.; Chen, Y. Atomically Precise Colloidal Metal Nanoclusters and Nanoparticles: Fundamentals and Opportunities. *Chemical Reviews* **2016**, *116*, 10346-10413, doi:10.1021/acs.chemrev.5b00703.
7. He, G.; Song, Y.; Liu, K.; Walter, A.; Chen, S.; Chen, S. Oxygen Reduction Catalyzed by Platinum Nanoparticles Supported on Graphene Quantum Dots. *ACS Catalysis* **2013**, *3*, 831-838, doi:10.1021/cs400114s.
8. Vázquez-González, M.; Liao, W.-C.; Cazelles, R.; Wang, S.; Yu, X.; Gutkin, V.; Willner, I. Mimicking Horseradish Peroxidase Functions Using Cu2+-Modified Carbon Nitride Nanoparticles or Cu2+-Modified Carbon Dots as Heterogeneous Catalysts. *ACS Nano* **2017**, *11*, 3247-3253, doi:10.1021/acsnano.7b00352.
9. Yang, W.; Liu, X.; Yue, X.; Jia, J.; Guo, S. Bamboo-like Carbon Nanotube/Fe3C Nanoparticle Hybrids and Their Highly Efficient Catalysis for Oxygen Reduction. *Journal of the American Chemical Society* **2015**, *137*, 1436-1439, doi:10.1021/ja5129132.
10. Fukuoka, A.; Higashimoto, N.; Sakamoto, Y.; Inagaki, S.; Fukushima, Y.; Ichikawa, M. Preparation and catalysis of Pt and Rh nanowires and particles in FSM-16. *Microporous Mesoporous Mater* **2001**, *48*, 171-179, doi:10.1016/S1387-1811(01)00341-9.
11. Luz, I.; Llabrés i Xamena, F.X.; Corma, A. Bridging homogeneous and heterogeneous catalysis with MOFs: "Click" reactions with Cu-MOF catalysts. *Journal of Catalysis* **2010**, *276*, 134-140, doi:10.1016/j.jcat.2010.09.010.
12. Zhou, Y.; Liu, B.; Yang, R.; Liu, J. Filling in the Gaps between Nanozymes and Enzymes: Challenges and Opportunities. *Bioconjug Chem* **2017**, *28*, 2903-2909, doi:10.1021/acs.bioconjchem.7b00673.
13. Huang, L.; Sun, D.W.; Pu, H.; Wei, Q. Development of Nanozymes for Food Quality and Safety Detection: Principles and Recent Applications. *Comprehensive Reviews in Food Science and Food Safety* **2019**, *18*, 1496-1513, doi:10.1111/1541-4337.12485.
14. Qiu, H.; Pu, F.; Ran, X.; Liu, C.; Ren, J.; Qu, X. Nanozyme as Artificial Receptor with Multiple Readouts for Pattern Recognition. *Analytical Chemistry* **2018**, *90*, 11775-11779, doi:10.1021/acs.analchem.8b03807.
15. Wei, D.; Zhang, X.; Chen, B.; Zeng, K. Using bimetallic Au@Pt nanozymes as a visual tag and as an enzyme mimic in enhanced sensitive lateral-flow immunoassays: Application for the detection of streptomycin. *Analytica Chimica Acta* **2020**, *1126*, 106-113, doi:10.1016/j.aca.2020.06.009.
16. Tian, L.; Qi, J.; Qian, K.; Oderinde, O.; Cai, Y.; Yao, C.; Song, W.; Wang, Y. An ultrasensitive electrochemical cytosensor based on the magnetic field assisted binanozymes synergistic catalysis of Fe3O4 nanozyme and reduced graphene oxide/molybdenum disulfide nanozyme. *Sensors and Actuators B: Chemical* **2018**, *260*, 676-684, doi:10.1016/j.snb.2018.01.092.
17. Liu, B.; Han, X.; Liu, J. Iron oxide nanozyme catalyzed synthesis of fluorescent polydopamine for light-up Zn2+ detection. *Nanoscale* **2016**, *8*, 13620-13626, doi:10.1039/C6NR02584F.
18. Sun, J.; Li, C.; Qi, Y.; Guo, S.; Liang, X. Optimizing Colorimetric Assay Based on V2O5 Nanozymes for Sensitive Detection of H2O2 and Glucose. *Sensors* **2016**, *16*, 584, doi:10.3390/s16040584.

19. Zhong, Y.; Tang, X.; Li, J.; Lan, Q.; Min, L.; Ren, C.; Hu, X.; Torrente-Rodríguez, R.M.; Gao, W.; Yang, Z. A nanozyme tag enabled chemiluminescence imaging immunoassay for multiplexed cytokine monitoring. *Chemical Communications* **2018**, *54*, 13813-13816, doi:10.1039/C8CC07779G.
20. Kong, W.; Guo, X.; Jing, M.; Qu, F.; Lu, L. Highly sensitive photoelectrochemical detection of bleomycin based on Au/WS2 nanorod array as signal matrix and Ag/ZnMOF nanozyme as multifunctional amplifier. *Biosens Bioelectron* **2020**, *150*, 111875, doi:10.1016/j.bios.2019.111875.
21. Sharma, T.K.; Ramanathan, R.; Weerathunge, P.; Mohammadtaheri, M.; Daima, H.K.; Shukla, R.; Bansal, V. Aptamer-mediated 'turn-off/turn-on' nanozyme activity of gold nanoparticles for kanamycin detection. *Chemical Communications* **2014**, *50*, 15856-15859, doi:10.1039/C4CC07275H.
22. Han, K.N.; Choi, J.-S.; Kwon, J. Gold nanozyme-based paper chip for colorimetric detection of mercury ions. *Scientific Reports* **2017**, *7*, 2806, doi:10.1038/s41598-017-02948-x.
23. Mirhosseini, M.; Shekari-Far, A.; Hakimian, F.; Haghiralsadat, B.F.; Fatemi, S.K.; Dashtestani, F. Core-shell Au@Co-Fe hybrid nanoparticles as peroxidase mimetic nanozyme for antibacterial application. *Process Biochemistry* **2020**, *95*, 131-138, doi:10.1016/j.procbio.2020.05.003.
24. Feng, L.; Liu, B.; Xie, R.; Wang, D.; Qian, C.; Zhou, W.; Liu, J.; Jana, D.; Yang, P.; Zhao, Y. An Ultrasmall SnFe2O4 Nanozyme with Endogenous Oxygen Generation and Glutathione Depletion for Synergistic Cancer Therapy. *Advanced Functional Materials* **2021**, *31*, 2006216, doi:10.1002/adfm.202006216.
25. Ren, L.; Deng, S.; Chu, Y.; Zhang, Y.; Zhao, H.; Chen, H.; Zhang, D. Single-wall carbon nanotubes improve cell survival rate and reduce oxidative injury in cryopreservation of Agapanthus praecox embryogenic callus. *Plant Methods* **2020**, *16*, 130, doi:10.1186/s13007-020-00674-6.
26. Wang, Y.; Liang, M.; Wei, T. Types of Nanozymes: Materials and Activities. In *Nanozymology*, Yan, X., Ed. Springer Singapore: Singapore, 2020; 10.1007/978-981-15-1490-6_3pp. 41-77.
27. Jain, P.K.; Huang, X.; El-Sayed, I.H.; El-Sayed, M.A. Noble Metals on the Nanoscale: Optical and Photothermal Properties and Some Applications in Imaging, Sensing, Biology, and Medicine. *Accounts of Chemical Research* **2008**, *41*, 1578-1586, doi:10.1021/ar7002804.
28. Sharifi, M.; Hosseinali, S.H.; Yousefvand, P.; Salihi, A.; Shekha, M.S.; Aziz, F.M.; JouyaTalaei, A.; Hasan, A.; Falahati, M. Gold nanozyme: Biosensing and therapeutic activities. *Materials Science and Engineering: C* **2020**, *108*, 110422, doi:10.1016/j.msec.2019.110422.
29. Liu, Y.; Ding, D.; Zhen, Y.; Guo, R. Amino acid-mediated 'turn-off/turn-on' nanozyme activity of gold nanoclusters for sensitive and selective detection of copper ions and histidine. *Biosens Bioelectron* **2017**, *92*, 140-146, doi:10.1016/j.bios.2017.01.036.
30. Yang, L.; Kim, T.-H.; Cho, H.-Y.; Luo, J.; Lee, J.-M.; Chueng, S.-T.D.; Hou, Y.; Yin, P.T.-T.; Han, J.; Kim, J.H., et al. Hybrid Graphene-Gold Nanoparticle-Based Nucleic Acid Conjugates for Cancer-Specific Multimodal Imaging and Combined Therapeutics. *Advanced Functional Materials* **2021**, *31*, 2006918, doi:10.1002/adfm.202006918.
31. Jv, Y.; Li, B.; Cao, R. Positively-charged gold nanoparticles as peroxidiase mimic and their application in hydrogen peroxide and glucose detection. *Chemical Communications* **2010**, *46*, 8017-8019, doi:10.1039/C0CC02698K.
32. Tao, Y.; Lin, Y.; Huang, Z.; Ren, J.; Qu, X. Incorporating Graphene Oxide and Gold Nanoclusters: A Synergistic Catalyst with Surprisingly High Peroxidase-Like Activity Over a Broad pH Range and its Application for Cancer Cell Detection. *Advanced Materials* **2013**, *25*, 2594-2599, doi:10.1002/adma.201204419.
33. Degliangeli, F.; Kshirsagar, P.; Brunetti, V.; Pompa, P.P.; Fiammengo, R. Absolute and Direct MicroRNA Quantification Using DNA–Gold Nanoparticle Probes. *Journal of the American Chemical Society* **2014**, *136*, 2264-2267, doi:10.1021/ja412152x.

34. Wang, Q.; Liu, R.; Yang, X.; Wang, K.; Zhu, J.; He, L.; Li, Q. Surface plasmon resonance biosensor for enzyme-free amplified microRNA detection based on gold nanoparticles and DNA supersandwich. *Sensors and Actuators B: Chemical* **2016**, *223*, 613-620, doi:10.1016/j.snb.2015.09.152.
35. Wei, Z.; Yu, Y.; Hu, S.; Yi, X.; Wang, J. Bifunctional Diblock DNA-Mediated Synthesis of Nanoflower-Shaped Photothermal Nanozymes for a Highly Sensitive Colorimetric Assay of Cancer Cells. *ACS Applied Materials & Interfaces* **2021**, *13*, 16801-16811, doi:10.1021/acsami.0c21109.
36. Tian, Y.; Chen, Y.; Chen, M.; Song, Z.-L.; Xiong, B.; Zhang, X.-B. Peroxidase-like Au@Pt nanozyme as an integrated nanosensor for Ag+ detection by LSPR spectroscopy. *Talanta* **2021**, *221*, 121627, doi:10.1016/j.talanta.2020.121627.
37. Zhang, M.-h.; Dong, H.; Zhao, L.; Wang, D.-x.; Meng, D. A review on Fenton process for organic wastewater treatment based on optimization perspective. *Science of The Total Environment* **2019**, *670*, 110-121, doi:10.1016/j.scitotenv.2019.03.180.
38. Ding, C.; Yan, Y.; Xiang, D.; Zhang, C.; Xian, Y. Magnetic Fe 3 S 4 nanoparticles with peroxidase-like activity, and their use in a photometric enzymatic glucose assay. *Microchimica Acta* **2016**, *183*, 625-631, doi:10.1007/s00604-015-1690-6.
39. Komkova, M.A.; Karyakina, E.E.; Karyakin, A.A. Catalytically Synthesized Prussian Blue Nanoparticles Defeating Natural Enzyme Peroxidase. *Journal of the American Chemical Society* **2018**, *140*, 11302-11307, doi:10.1021/jacs.8b05223.
40. Vlasova, K.Y.; Vishwasrao, H.; Abakumov, M.A.; Golovin, D.Y.; Gribanovsky, S.L.; Zhigachev, A.O.; Poloznikov, A.A.; Majouga, A.G.; Golovin, Y.I.; Sokolsky-Papkov, M., et al. Enzyme Release from Polyion Complex by Extremely Low Frequency Magnetic Field. *Scientific Reports* **2020**, *10*, 4745, doi:10.1038/s41598-020-61364-w.
41. Farhana, F.Z.; Umer, M.; Saeed, A.; Pannu, A.S.; Shahbazi, M.; Jabur, A.; Nam, H.J.; Ostrikov, K.; Sonar, P.; Firoz, S.H., et al. Isolation and Detection of Exosomes Using Fe2O3 Nanoparticles. *ACS Applied Nano Materials* **2021**, 10.1021/acsanm.0c02807, doi:10.1021/acsanm.0c02807.
42. Wang, M.; Wang, N.; Tang, H.; Cao, M.; She, Y.; Zhu, L. Surface modification of nano-Fe3O4 with EDTA and its use in H2O2 activation for removing organic pollutants. *Catalysis Science & Technology* **2012**, *2*, 187-194, doi:10.1039/C1CY00260K.
43. Senapati, V.A.; Jain, A.K.; Gupta, G.S.; Pandey, A.K.; Dhawan, A. Chromium oxide nanoparticle-induced genotoxicity and p53-dependent apoptosis in human lung alveolar cells. *Journal of Applied Toxicology* **2015**, *35*, 1179-1188, doi:10.1002/jat.3174.
44. Moche, H.; Chevalier, D.; Vezin, H.; Claude, N.; Lorge, E.; Nesslany, F. Genotoxicity of tungsten carbide–cobalt (WC–Co) nanoparticles in vitro: Mechanisms-of-action studies. *Mutation Research/Genetic Toxicology and Environmental Mutagenesis* **2015**, *779*, 15-22, doi:10.1016/j.mrgentox.2015.02.002.
45. Xu, L.; Yang, Y.; Li, W.; Tao, Y.; Sui, Z.; Song, S.; Yang, J. Three-dimensional macroporous graphene-wrapped zero-valent copper nanoparticles as efficient micro-electrolysis-promoted Fenton-like catalysts for metronidazole removal. *Science of The Total Environment* **2019**, *658*, 219-233, doi:10.1016/j.scitotenv.2018.12.040.
46. Tušar, N.N.; Maučec, D.; Rangus, M.; Arčon, I.; Mazaj, M.; Cotman, M.; Pintar, A.; Kaučič, V. Manganese Functionalized Silicate Nanoparticles as a Fenton-Type Catalyst for Water Purification by Advanced Oxidation Processes (AOP). *Advanced Functional Materials* **2012**, *22*, 820-826, doi:10.1002/adfm.201102361.
47. Hu, Z.; Leung, C.-F.; Tsang, Y.-K.; Du, H.; Liang, H.; Qiu, Y.; Lau, T.-C. A recyclable polymer-supported ruthenium catalyst for the oxidative degradation of bisphenol A in water using hydrogen peroxide. *New Journal of Chemistry* **2011**, *35*, 149-155, doi:10.1039/C0NJ00583E.
48. Bokare, A.D.; Choi, W. Review of iron-free Fenton-like systems for activating H2O2 in advanced oxidation processes. *J Hazard Mater* **2014**, *275*, 121-135, doi:10.1016/j.jhazmat.2014.04.054.
49. Gordijo, C.R.; Abbasi, A.Z.; Amini, M.A.; Lip, H.Y.; Maeda, A.; Cai, P.; O'Brien, P.J.; DaCosta, R.S.; Rauth, A.M.; Wu, X.Y. Design of Hybrid MnO2-Polymer-Lipid Nanoparticles with Tunable Oxygen Generation Rates and Tumor Accumulation for Cancer Treatment. *Advanced Functional Materials* **2015**, *25*, 1858-1872, doi:10.1002/adfm.201404511.

50. Du, W.; Liu, T.; Xue, F.; Chen, Y.; Chen, Q.; Luo, Y.; Cai, X.; Ma, M.; Chen, H. Confined nanoparticles growth within hollow mesoporous nanoreactors for highly efficient MRI-guided photodynamic therapy. *Chemical Engineering Journal* **2020**, *379*, 122251, doi:10.1016/j.cej.2019.122251.
51. Zhang, Y.; Wang, Y.; Huang, J.; Han, C.; Zang, J. Mn3O4 nanosheets coated on carbon nanotubes as efficient electrocatalysts for oxygen reduction reaction. *International Journal of Hydrogen Energy* **2020**, *45*, 6529-6537, doi:10.1016/j.ijhydene.2019.12.216.
52. Pranudta, A.; Klysubun, W.; El-Moselhy, M.M.; Padungthon, S. Synthesis optimization and X-ray absorption spectroscopy investigation of polymeric anion exchanger supported binary Fe/Mn oxides nanoparticles for enhanced As(III) removal. *Reactive and Functional Polymers* **2020**, *147*, 104441, doi:10.1016/j.reactfunctpolym.2019.104441.
53. Guo, S.-y.; Sun, D.; Ni, D.-l.; Yu, M.-r.; Qian, K.; Zhang, W.; Yang, Y.-w.; Song, S.; Li, Y.; Xi, Z.-y., et al. Smart Tumor Microenvironment-Responsive Nanotheranostic Agent for Effective Cancer Therapy. *Advanced Functional Materials* **2020**, *n/a*, 2000486, doi:10.1002/adfm.202000486.
54. Tian, L.; Qi, J.; Qian, K.; Oderinde, O.; Liu, Q.; Yao, C.; Song, W.; Wang, Y. Copper (II) oxide nanozyme based electrochemical cytosensor for high sensitive detection of circulating tumor cells in breast cancer. *Journal of Electroanalytical Chemistry* **2018**, *812*, 1-9, doi:10.1016/j.jelechem.2017.12.012.
55. Dai, D.; Liu, H.; Ma, H.; Huang, Z.; Gu, C.; Zhang, M. In-situ synthesis of Cu2OAu nanocomposites as nanozyme for colorimetric determination of hydrogen peroxide. *Journal of Alloys and Compounds* **2018**, *747*, 676-683, doi:10.1016/j.jallcom.2018.03.054.
56. Zen, J.-M.; Chung, H.-H.; Kumar, A.S. Flow injection analysis of hydrogen peroxide on copper-plated screen-printed carbon electrodes. *Analyst* **2000**, *125*, 1633-1637, doi:10.1039/B004207M.
57. Tranchemontagne, D.J.; Mendoza-Cortés, J.L.; O'Keeffe, M.; Yaghi, O.M. Secondary building units, nets and bonding in the chemistry of metal–organic frameworks. *Chemical Society Reviews* **2009**, *38*, 1257-1283, doi:10.1039/B817735J.
58. Zhou, H.-C.; Long, J.R.; Yaghi, O.M. Introduction to Metal–Organic Frameworks. *Chemical Reviews* **2012**, *112*, 673-674, doi:10.1021/cr300014x.
59. Chen, B.; Xiang, S.; Qian, G. Metal–Organic Frameworks with Functional Pores for Recognition of Small Molecules. *Accounts of Chemical Research* **2010**, *43*, 1115-1124, doi:10.1021/ar100023y.
60. Hu, Z.; Deibert, B.J.; Li, J. Luminescent metal–organic frameworks for chemical sensing and explosive detection. *Chemical Society Reviews* **2014**, *43*, 5815-5840, doi:10.1039/C4CS00010B.
61. Rocha, J.; Carlos, L.D.; Paz, F.A.A.; Ananias, D. Luminescent multifunctional lanthanides-based metal–organic frameworks. *Chemical Society Reviews* **2011**, *40*, 926-940, doi:10.1039/C0CS00130A.
62. Wang, B.; Luo, Y.; Gao, L.; Liu, B.; Duan, G. High-performance field-effect transistor glucose biosensors based on bimetallic Ni/Cu metal-organic frameworks. *Biosens Bioelectron* **2021**, *171*, 112736, doi:10.1016/j.bios.2020.112736.
63. Lin, C.; Du, Y.; Wang, S.; Wang, L.; Song, Y. Glucose oxidase@Cu-hemin metal-organic framework for colorimetric analysis of glucose. *Materials Science and Engineering: C* **2021**, *118*, 111511, doi:10.1016/j.msec.2020.111511.
64. Zhao, M.; Huang, Z.; Wang, S.; Zhang, L.; Zhou, Y. Design of l-Cysteine Functionalized UiO-66 MOFs for Selective Adsorption of Hg(II) in Aqueous Medium. *ACS Applied Materials & Interfaces* **2019**, *11*, 46973-46983, doi:10.1021/acsami.9b17508.
65. Zheng, H.-Q.; Zeng, Y.-N.; Chen, J.; Lin, R.-G.; Zhuang, W.-E.; Cao, R.; Lin, Z.-J. Zr-Based Metal–Organic Frameworks with Intrinsic Peroxidase-Like Activity for Ultradeep Oxidative Desulfurization: Mechanism of H2O2 Decomposition. *Inorganic Chemistry* **2019**, *58*, 6983-6992, doi:10.1021/acs.inorgchem.9b00604.

66. Xu, W.; Kang, Y.; Jiao, L.; Wu, Y.; Yan, H.; Li, J.; Gu, W.; Song, W.; Zhu, C. Tuning Atomically Dispersed Fe Sites in Metal–Organic Frameworks Boosts Peroxidase-Like Activity for Sensitive Biosensing. *Nano-Micro Letters* **2020**, *12*, 184, doi:10.1007/s40820-020-00520-3.
67. Huang, L.; Chen, J.; Gan, L.; Wang, J.; Dong, S. Single-atom nanozymes. *Science Advances* **2019**, *5*, eaav5490, doi:10.1126/sciadv.aav5490.
68. Ding, H.; Hu, B.; Zhang, B.; Zhang, H.; Yan, X.; Nie, G.; Liang, M. Carbon-based nanozymes for biomedical applications. *Nano Research* **2021**, *14*, 570-583, doi:10.1007/s12274-020-3053-9.
69. Sun, H.; Zhou, Y.; Ren, J.; Qu, X. Carbon Nanozymes: Enzymatic Properties, Catalytic Mechanism, and Applications. *Angewandte Chemie International Edition* **2018**, *57*, 9224-9237, doi:10.1002/anie.201712469.
70. Garg, B.; Bisht, T. Carbon Nanodots as Peroxidase Nanozymes for Biosensing. *Molecules* **2016**, *21*, 1653, doi:10.3390/molecules21121653.
71. Sun, H.; Zhou, Y.; Ren, J.; Qu, X. Carbon Nanozymes: Enzymatic Properties, Catalytic Mechanism, and Applications. *Angew Chem Int Ed Engl* **2018**, *57*, 9224-9237, doi:10.1002/anie.201712469.
72. Joshi, S.; Sharma, P.; Siddiqui, R.; Kaushal, K.; Sharma, S.; Verma, G.; Saini, A. A review on peptide functionalized graphene derivatives as nanotools for biosensing. *Mikrochim Acta* **2019**, *187*, 27, doi:10.1007/s00604-019-3989-1.
73. Song, Y.; Qu, K.; Zhao, C.; Ren, J.; Qu, X. Graphene Oxide: Intrinsic Peroxidase Catalytic Activity and Its Application to Glucose Detection. *Advanced Materials* **2010**, *22*, 2206-2210, doi:10.1002/adma.200903783.
74. Dang, W.; Sun, Y.; Jiao, H.; Xu, L.; Lin, M. AuNPs-NH2/Cu-MOF modified glassy carbon electrode as enzyme-free electrochemical sensor detecting H2O2. *Journal of Electroanalytical Chemistry* **2020**, *856*, 113592, doi:10.1016/j.jelechem.2019.113592.
75. Wang, D.; Wu, H.; Phua, S.Z.F.; Yang, G.; Qi Lim, W.; Gu, L.; Qian, C.; Wang, H.; Guo, Z.; Chen, H., et al. Self-assembled single-atom nanozyme for enhanced photodynamic therapy treatment of tumor. *Nature Communications* **2020**, *11*, 357, doi:10.1038/s41467-019-14199-7.
76. Shah, S.N.A.; Dou, X.; Khan, M.; Uchiyama, K.; Lin, J.-M. N-doped carbon dots/H2O2 chemiluminescence system for selective detection of Fe2+ ion in environmental samples. *Talanta* **2019**, *196*, 370-375, doi:10.1016/j.talanta.2018.12.091.
77. Jin, S.; Wu, C.; Ying, Y.; Ye, Z. Magnetically separable and recyclable bamboo-like carbon nanotube–based FRET assay for sensitive and selective detection of Hg2+. *Analytical and Bioanalytical Chemistry* **2020**, 10.1007/s00216-020-02631-7, 3779-3786, doi:10.1007/s00216-020-02631-7.
78. Kudr, J.; Richtera, L.; Xhaxhiu, K.; Hynek, D.; Heger, Z.; Zitka, O.; Adam, V. Carbon dots based FRET for the detection of DNA damage. *Biosensors and Bioelectronics* **2017**, *92*, 133-139, doi:10.1016/j.bios.2017.01.067.
79. Li, Z.-M.; Pi, T.; Yan, X.-L.; Tang, X.-M.; Deng, R.-H.; Zheng, X.-J. Label-free and enzyme-free one-step rapid colorimetric detection of DNA methylation based on unmodified gold nanoparticles. *Spectrochimica Acta Part A: Molecular and Biomolecular Spectroscopy* **2020**, 10.1016/j.saa.2020.118375, 118375, doi:10.1016/j.saa.2020.118375.
80. Wang, Y.-M.; Liu, J.-W.; Adkins, G.B.; Shen, W.; Trinh, M.P.; Duan, L.-Y.; Jiang, J.-H.; Zhong, W. Enhancement of the Intrinsic Peroxidase-Like Activity of Graphitic Carbon Nitride Nanosheets by ssDNAs and Its Application for Detection of Exosomes. *Analytical chemistry* **2017**, *89*, 12327-12333, doi:10.1021/acs.analchem.7b03335.
81. Fan, K.; Xi, J.; Fan, L.; Wang, P.; Zhu, C.; Tang, Y.; Xu, X.; Liang, M.; Jiang, B.; Yan, X., et al. In vivo guiding nitrogen-doped carbon nanozyme for tumor catalytic therapy. *Nature Communications* **2018**, *9*, 1440, doi:10.1038/s41467-018-03903-8.
82. Khan, A.A.; Rahmani, A.H.; Aldebasi, Y.H.; Aly, S.M. Biochemical and pathological studies on peroxidases -an updated review. *Glob J Health Sci* **2014**, *6*, 87-98, doi:10.5539/gjhs.v6n5p87.

83. Sun, H.; Zhao, A.; Gao, N.; Li, K.; Ren, J.; Qu, X. Deciphering a Nanocarbon-Based Artificial Peroxidase: Chemical Identification of the Catalytically Active and Substrate-Binding Sites on Graphene Quantum Dots. *Angewandte Chemie International Edition* **2015**, *54*, 7176-7180, doi:10.1002/anie.201500626.
84. Zhao, R.; Zhao, X.; Gao, X. Molecular-Level Insights into Intrinsic Peroxidase-Like Activity of Nanocarbon Oxides. *Chemistry – A European Journal* **2015**, *21*, 960-964, doi:10.1002/chem.201404647.
85. Xie, X.; Wang, Y.; Zhou, X.; Chen, J.; Wang, M.; Su, X. Fe-N-C single-atom nanozymes with peroxidase-like activity for the detection of alkaline phosphatase. *Analyst* **2021**, *146*, 896-903, doi:10.1039/d0an01846e.
86. Wang, J.; Hu, Y.; Zhou, Q.; Hu, L.; Fu, W.; Wang, Y. Peroxidase-like Activity of Metal-Organic Framework [Cu(PDA)(DMF)] and Its Application for Colorimetric Detection of Dopamine. *ACS Appl Mater Interfaces* **2019**, *11*, 44466-44473, doi:10.1021/acsami.9b17488.
87. Li, J.; Zhao, J.; Li, S.; Chen, Y.; Lv, W.; Zhang, J.; Zhang, L.; Zhang, Z.; Lu, X. Synergistic effect enhances the peroxidase-like activity in platinum nanoparticle-supported metal—organic framework hybrid nanozymes for ultrasensitive detection of glucose. *Nano Research* **2021**, 10.1007/s12274-021-3406-z, doi:10.1007/s12274-021-3406-z.
88. Mazhani, M.; Alula, M.T.; Murape, D. Development of a cysteine sensor based on the peroxidase-like activity of AgNPs@ Fe3O4 core-shell nanostructures. *Analytica Chimica Acta* **2020**, *1107*, 193-202, doi:https://doi.org/10.1016/j.aca.2020.02.021.
89. Lu, W.; Yuan, M.; Chen, J.; Zhang, J.; Kong, L.; Feng, Z.; Ma, X.; Su, J.; Zhan, J. Synergistic Lewis acid-base sites of ultrathin porous Co3O4 nanosheets with enhanced peroxidase-like activity. *Nano Research* **2021**, 10.1007/s12274-021-3656-9, doi:10.1007/s12274-021-3656-9.
90. Zhou, X.; Wang, M.; Chen, J.; Xie, X.; Su, X. Peroxidase-like activity of Fe-N-C single-atom nanozyme based colorimetric detection of galactose. *Anal Chim Acta* **2020**, *1128*, 72-79, doi:10.1016/j.aca.2020.06.027.
91. Tian, Y.; Chen, Y.; Chen, M.; Song, Z.L.; Xiong, B.; Zhang, X.B. Peroxidase-like Au@Pt nanozyme as an integrated nanosensor for Ag(+) detection by LSPR spectroscopy. *Talanta* **2021**, *221*, 121627, doi:10.1016/j.talanta.2020.121627.
92. Chen, Q.; Liu, Y.; Liu, J.; Liu, J. Liposome-Boosted Peroxidase-Mimicking Nanozymes Breaking the pH Limit. *Chemistry (Weinheim an der Bergstrasse, Germany)* **2020**, *26*, 16659-16665, doi:10.1002/chem.202004133.
93. Zhao, L.; Wang, J.; Su, D.; Zhang, Y.; Lu, H.; Yan, X.; Bai, J.; Gao, Y.; Lu, G. The DNA controllable peroxidase mimetic activity of MoS(2) nanosheets for constructing a robust colorimetric biosensor. *Nanoscale* **2020**, *12*, 19420-19428, doi:10.1039/d0nr05649a.
94. Shih, J.C.; Chen, K.; Ridd, M.J. MONOAMINE OXIDASE: From Genes to Behavior. *Annual Review of Neuroscience* **1999**, *22*, 197-217, doi:10.1146/annurev.neuro.22.1.197.
95. Babior, B.M. NADPH oxidase. *Current opinion in immunology* **2004**, *16*, 42-47, doi:10.1016/j.coi.2003.12.001.
96. Wang, Q.; Warelow, T.P.; Kang, Y.-S.; Romano, C.; Osborne, T.H.; Lehr, C.R.; Bothner, B.; McDermott, T.R.; Santini, J.M.; Wang, G. Arsenite oxidase also functions as an antimonite oxidase. *Appl Environ Microbiol* **2015**, *81*, 1959-1965, doi:10.1128/AEM.02981-14.
97. Comotti, M.; Della Pina, C.; Falletta, E.; Rossi, M. Aerobic Oxidation of Glucose with Gold Catalyst: Hydrogen Peroxide as Intermediate and Reagent. *Advanced Synthesis & Catalysis* **2006**, *348*, 313-316, doi:10.1002/adsc.200505389.
98. Lin, Z.; Zhang, X.; Liu, S.; Zheng, L.; Bu, Y.; Deng, H.; Chen, R.; Peng, H.; Lin, X.; Chen, W. Colorimetric acid phosphatase sensor based on MoO3 nanozyme. *Analytica Chimica Acta* **2020**, *1105*, 162-168, doi:10.1016/j.aca.2020.01.035.
99. Xu, C.; Qu, X. Cerium oxide nanoparticle: a remarkably versatile rare earth nanomaterial for biological applications. *NPG Asia Materials* **2014**, *6*, e90-e90, doi:10.1038/am.2013.88.
100. Celardo, I.; Pedersen, J.Z.; Traversa, E.; Ghibelli, L. Pharmacological potential of cerium oxide nanoparticles. *Nanoscale* **2011**, *3*, 1411-1420, doi:10.1039/C0NR00875C.

101. Yıldırım, D.; Gökçal, B.; Büber, E.; Kip, Ç.; Demir, M.C.; Tuncel, A. A new nanozyme with peroxidase-like activity for simultaneous phosphoprotein isolation and detection based on metal oxide affinity chromatography: Monodisperse-porous cerium oxide microspheres. *Chemical Engineering Journal* **2021**, *403*, 126357, doi:10.1016/j.cej.2020.126357.
102. Liu, X.; Wang, Y.; Chen, P.; McCadden, A.; Palaniappan, A.; Zhang, J.; Liedberg, B. Peptide Functionalized Gold Nanoparticles with Optimized Particle Size and Concentration for Colorimetric Assay Development: Detection of Cardiac Troponin I. *ACS Sensors* **2016**, *1*, 1416-1422, doi:10.1021/acssensors.6b00493.
103. Liu, B.; Liu, J. Surface modification of nanozymes. *Nano Research* **2017**, *10*, 1125-1148, doi:10.1007/s12274-017-1426-5.
104. Huo, J.; Hao, J.; Mu, J.; Wang, Y. Surface Modification of Co3O4 Nanoplates as Efficient Peroxidase Nanozymes for Biosensing Application. *ACS Applied Bio Materials* **2021**, *4*, 3443-3452, doi:10.1021/acsabm.1c00017.
105. Yang, D.; Fa, M.; Gao, L.; Zhao, R.; Luo, Y.; Yao, X. The effect of DNA on the oxidase activity of nanoceria with different morphologies. *Nanotechnology* **2018**, *29*, 385101, doi:10.1088/1361-6528/aacf86.
106. Wang, Z.; Zhang, R.; Yan, X.; Fan, K. Structure and activity of nanozymes: Inspirations for de novo design of nanozymes. *Materials Today* **2020**, *41*, 81-119, doi:10.1016/j.mattod.2020.08.020.
107. Wei, M.; Lee, J.; Xia, F.; Lin, P.; Hu, X.; Li, F.; Ling, D. Chemical design of nanozymes for biomedical applications. *Acta Biomaterialia* **2021**, *126*, 15-30, doi:10.1016/j.actbio.2021.02.036.
108. Yue, Y.; Wei, H.; Guo, J.; Yang, Y. Ceria-based peroxidase-mimicking nanozyme with enhanced activity: A coordination chemistry strategy. *Colloids and Surfaces A: Physicochemical and Engineering Aspects* **2021**, *610*, 125715, doi:10.1016/j.colsurfa.2020.125715.
109. Zhao, W.; Zhang, G.; du, y.; Chen, S.; Fu, Y.; Xu, F.; Xiao, X.; Jiang, W.; Ji, Q. Sensitive Colorimetric Glucose Sensor by Iron-based Nanozymes with Controllable Fe Valence. *Journal of Materials Chemistry B* **2021**, 10.1039/D1TB00370D, doi:10.1039/D1TB00370D.
110. Adegoke, O.; Zolotovskaya, S.; Abdolvand, A.; Daeid, N.N. Rapid and highly selective colorimetric detection of nitrite based on the catalytic-enhanced reaction of mimetic Au nanoparticle-CeO2 nanoparticle-graphene oxide hybrid nanozyme. *Talanta* **2021**, *224*, 121875, doi:10.1016/j.talanta.2020.121875.
111. Liu, B.; Wang, Y.; Chen, Y.; Guo, L.; Wei, G. Biomimetic two-dimensional nanozymes: synthesis, hybridization, functional tailoring, and biosensor applications. *Journal of Materials Chemistry B* **2020**, *8*, 10065-10086, doi:10.1039/D0TB02051F.
112. Wu, J.; Yang, Q.; Li, Q.; Li, H.; Li, F. Two-Dimensional MnO2 Nanozyme-Mediated Homogeneous Electrochemical Detection of Organophosphate Pesticides without the Interference of H2O2 and Color. *Analytical Chemistry* **2021**, *93*, 4084-4091, doi:10.1021/acs.analchem.0c05257.
113. Cai, S.; Fu, Z.; Xiao, W.; Xiong, Y.; Wang, C.; Yang, R. Zero-Dimensional/Two-Dimensional AuxPd100–x Nanocomposites with Enhanced Nanozyme Catalysis for Sensitive Glucose Detection. *ACS Applied Materials & Interfaces* **2020**, *12*, 11616-11624, doi:10.1021/acsami.9b21621.
114. Zhang, H. Ultrathin Two-Dimensional Nanomaterials. *ACS Nano* **2015**, *9*, 9451-9469, doi:10.1021/acsnano.5b05040.
115. Song, Z.; Jiang, C.; Wang, F.; Yu, L.; Ye, S.; Dramou, P.; He, H. Nanozyme based on graphene oxide modified with Fe3O4, CuO, and cucurbit[6]uril for colorimetric determination of homocysteine. *Microchimica Acta* **2021**, *188*, 207, doi:10.1007/s00604-021-04868-0.
116. Chang, M.; Hou, Z.; Wang, M.; Yang, C.; Wang, R.; Li, F.; Liu, D.; Peng, T.; Li, C.; Lin, J. Single-Atom Pd Nanozyme for Ferroptosis-Boosted Mild-Temperature Photothermal Therapy. *Angewandte Chemie International Edition* **2021**, *60*, 12971-12979, doi:10.1002/anie.202101924.
117. Zhu, J.; Luo, G.; Xi, X.; Wang, Y.; Selvaraj, J.N.; Wen, W.; Zhang, X.; Wang, S. Cu2+-modified hollow carbon nanospheres: an unusual nanozyme with enhanced peroxidase-like activity. *Microchimica Acta* **2021**, *188*, 8, doi:10.1007/s00604-020-04690-0.

118. Tian, R.; Sun, J.; Qi, Y.; Zhang, B.; Guo, S.; Zhao, M. Influence of VO2 Nanoparticle Morphology on the Colorimetric Assay of H2O2 and Glucose. *Nanomaterials* **2017**, *7*, doi:10.3390/nano7110347.
119. Zhu, M.; Dai, Y.; Wu, Y.; Liu, K.; Qi, X.; Sun, Y. Bandgap control of α-Fe2O3 nanozymes and their superior visible light promoted peroxidase-like catalytic activity. *Nanotechnology* **2018**, *29*, 465704.
120. Lu, C.; Tang, L.; Gao, F.; Li, Y.; Liu, J.; Zheng, J. DNA-encoded bimetallic Au-Pt dumbbell nanozyme for high-performance detection and eradication of Escherichia coli O157:H7. *Biosensors and Bioelectronics* **2021**, *187*, 113327, doi:10.1016/j.bios.2021.113327.
121. Liang, D.; Yang, Y.; Li, G.; Wang, Q.; Chen, H.; Deng, X. Endogenous H2O2-Sensitive and Weak Acidic pH-Triggered Nitrogen-Doped Graphene Nanoparticles (N-GNMs) in the Tumor Microenvironment Serve as Peroxidase-Mimicking Nanozymes for Tumor-Specific Treatment. *Materials* **2021**, *14*, 1933.
122. Gajendar, S.; Amisha, K.; Manu, S. Mildly acidic pH and room temperature triggered peroxidase-mimics of rGO–Cu3(OH)2(MoO4)2 cuboidal nanostructures: an effective colorimetric detection of neurotransmitter dopamine in blood serum and urine samples. *CrystEngComm* **2021**, *23*, 599-616, doi:10.1039/D0CE01423K.
123. Wang, X.; Shi, Q.; Zha, Z.; Zhu, D.; Zheng, L.; Shi, L.; Wei, X.; Lian, L.; Wu, K.; Cheng, L. Copper single-atom catalysts with photothermal performance and enhanced nanozyme activity for bacteria‐infected wound therapy. *Bioactive Materials* **2021**, *6*, 4389-4401, doi:10.1016/j.bioactmat.2021.04.024.
124. Li, Y.; Zhu, W.; Li, J.; Chu, H. Research progress in nanozyme-based composite materials for fighting against bacteria and biofilms. *Colloids and Surfaces B: Biointerfaces* **2021**, *198*, 111465, doi:10.1016/j.colsurfb.2020.111465.
125. Li, S.; Shang, L.; Xu, B.; Wang, S.; Gu, K.; Wu, Q.; Sun, Y.; Zhang, Q.; Yang, H.; Zhang, F., et al. A Nanozyme with Photo-Enhanced Dual Enzyme-Like Activities for Deep Pancreatic Cancer Therapy. *Angewandte Chemie International Edition* **2019**, *58*, 12624-12631, doi:10.1002/anie.201904751.
126. Singh, R.; Singh, S. Redox-dependent catalase mimetic cerium oxide-based nanozyme protect human hepatic cells from 3-AT induced acatalasemia. *Colloids and Surfaces B: Biointerfaces* **2019**, *175*, 625-635, doi:10.1016/j.colsurfb.2018.12.042.
127. Wang, Q.; Wei, H.; Zhang, Z.; Wang, E.; Dong, S. Nanozyme: An emerging alternative to natural enzyme for biosensing and immunoassay. *TrAC Trends in Analytical Chemistry* **2018**, *105*, 218-224, doi:10.1016/j.trac.2018.05.012.
128. Shukla, A.K.; Sharma, C.; Acharya, A. Bioinspired Metal-Free Fluorescent Carbon Nanozyme with Dual Catalytic Activity to Confront Cellular Oxidative Damage. *ACS Applied Materials & Interfaces* **2021**, *13*, 15040-15052, doi:10.1021/acsami.1c03130.
129. Liu, P.; Li, X.; Xu, X.; Ye, K.; Wang, L.; Zhu, H.; Wang, M.; Niu, X. Integrating peroxidase-mimicking activity with photoluminescence into one framework structure for high-performance ratiometric fluorescent pesticide sensing. *Sensors and Actuators B: Chemical* **2021**, *328*, 129024, doi:10.1016/j.snb.2020.129024.
130. Zhu, Y.; Liu, P.; Xue, T.; Xu, J.; Qiu, D.; Sheng, Y.; Li, W.; Lu, X.; Ge, Y.; Wen, Y. Facile and rapid one-step mass production of flexible 3D porous graphene nanozyme electrode via direct laser-writing for intelligent evaluation of fish freshness. *Microchemical Journal* **2021**, *162*, 105855, doi:10.1016/j.microc.2020.105855.
131. Adeel, M.; Canzonieri, V.; Daniele, S.; Vomiero, A.; Rizzolio, F.; Rahman, M.M. 2D metal azolate framework as nanozyme for amperometric detection of glucose at physiological pH and alkaline medium. *Microchimica Acta* **2021**, *188*, 77, doi:10.1007/s00604-021-04737-w.
132. Pavlaki, M.D.; Morgado, R.G.; Ferreira, V.; Rocha, R.J.; Soares, A.M.; Calado, R.; Loureiro, S. Cadmium Accumulation and Kinetics in Solea senegalensis Tissues under Dietary and Water Exposure and the Link to Human Health. *Water* **2021**, *13*, 522.
133. Ullah, I.; Zhao, L.; Hai, Y.; Fahim, M.; Alwayli, D.; Wang, X.; Li, H. Metal elements and pesticides as risk factors for Parkinson's disease - A review. *Toxicology Reports* **2021**, *8*, 607-616, doi:10.1016/j.toxrep.2021.03.009.

134. Wong, E.L.S.; Vuong, K.Q.; Chow, E. Nanozymes for Environmental Pollutant Monitoring and Remediation. *Sensors* **2021**, *21*, doi:10.3390/s21020408.
135. Zhang, L.; Han, Y.; Zhao, F.; Shi, G.; Tian, Y. A selective and accurate ratiometric electrochemical biosensor for monitoring of Cu2+ ions in a rat brain. *Anal Chem* **2015**, *87*, 2931-2936, doi:10.1021/ac504448m.
136. Hu Xue, F.; Singh, K.; Chan Hing, M. Mercury Exposure, Blood Pressure, and Hypertension: A Systematic Review and Dose–response Meta-analysis. *Environmental Health Perspectives* **2018**, *126*, 076002, doi:10.1289/EHP2863.
137. Logan, N.; McVey, C.; Elliott, C.; Cao, C. Amalgamated gold-nanoalloys with enhanced catalytic activity for the detection of mercury ions (Hg2+) in seawater samples. *Nano Research* **2020**, *13*, 989-998, doi:10.1007/s12274-020-2731-y.
138. Zheng, F.; Ke, W.; Zhao, Y.; Xu, C. Pt NPs catalyzed chemiluminescence method for Hg2+ detection based on a flow injection system. *ELECTROPHORESIS* **2019**, *40*, 2218-2226, doi:10.1002/elps.201900014.
139. Song, C.; Li, J.; Sun, Y.; Jiang, X.; Zhang, J.; Dong, C.; Wang, L. Colorimetric/SERS dual-mode detection of mercury ion via SERS-Active peroxidase-like Au@AgPt NPs. *Sensors and Actuators B: Chemical* **2020**, *310*, 127849, doi:10.1016/j.snb.2020.127849.
140. Langer, J.; Jimenez de Aberasturi, D.; Aizpurua, J.; Alvarez-Puebla, R.A.; Auguié, B.; Baumberg, J.J.; Bazan, G.C.; Bell, S.E.J.; Boisen, A.; Brolo, A.G., et al. Present and Future of Surface-Enhanced Raman Scattering. *ACS Nano* **2020**, *14*, 28-117, doi:10.1021/acsnano.9b04224.
141. Lu, Z.; Dang, Y.; Dai, C.; Zhang, Y.; Zou, P.; Du, H.; Zhang, Y.; Sun, M.; Rao, H.; Wang, Y. Hollow MnFeO oxide derived from MOF@MOF with multiple enzyme-like activities for multifunction colorimetric assay of biomolecules and Hg2+. *Journal of Hazardous Materials* **2021**, *403*, 123979, doi:10.1016/j.jhazmat.2020.123979.
142. Festa, R.A.; Thiele, D.J. Copper: an essential metal in biology. *Curr Biol* **2011**, *21*, R877-R883, doi:10.1016/j.cub.2011.09.040.
143. Tapiero, H.; Townsend, D.M.; Tew, K.D. Trace elements in human physiology and pathology. Copper. *Biomed Pharmacother* **2003**, *57*, 386-398, doi:10.1016/s0753-3322(03)00012-x.
144. Johncilla, M.; Mitchell, K.A. Pathology of the Liver in Copper Overload. *Seminars in Liver Disease* **2011**, *31*, 239-244, doi:10.1055/s-0031-1286055.
145. Gao, B.; Chen, D.; Gu, B.; Wang, T.; Wang, Z.; xie, F.; Yang, Y.; Guo, Q.; Wang, G. Facile and highly effective synthesis of nitrogen-doped graphene quantum dots as a fluorescent sensing probe for Cu2+ detection. *Current Applied Physics* **2020**, *20*, 538-544, doi:10.1016/j.cap.2020.01.018.
146. Falcone, E.; Gonzalez, P.; Lorusso, L.; Sénèque, O.; Faller, P.; Raibaut, L. A terbium(iii) luminescent ATCUN-based peptide sensor for selective and reversible detection of copper(ii) in biological media. *Chemical Communications* **2020**, *56*, 4797-4800, doi:10.1039/D0CC01007C.
147. Blanc, A.; Pandey, N.R.; Srivastava, A.K. Synchronous activation of ERK 1/2, p38mapk and PKB/Akt signaling by H2O2 in vascular smooth muscle cells: potential involvement in vascular disease. *Int. J. Molec. Med.* **2003**, *11*, 229-234, doi:10.3892/ijmm.11.2.229.
148. Wang, X.; Qin, L.; Lin, M.; Xing, H.; Wei, H. Fluorescent Graphitic Carbon Nitride-Based Nanozymes with Peroxidase-Like Activities for Ratiometric Biosensing. *Anal Chem* **2019**, *91*, 10648-10656, doi:10.1021/acs.analchem.9b01884.
149. Liu, B.; Liu, J. Molecular Detection Using Nanozymes. In *Nanozymology: Connecting Biology and Nanotechnology*, Yan, X., Ed. Springer Singapore: Singapore, 2020; 10.1007/978-981-15-1490-6_12pp. 395-424.
150. Nie, F.; Ga, L.; Ai, J.; Wang, Y. Trimetallic PdCuAu Nanoparticles for Temperature Sensing and Fluorescence Detection of H2O2 and Glucose. *Frontiers in Chemistry* **2020**, *8*, 244, doi:10.3389/fchem.2020.00244.
151. Chen, J.; Gao, H.; Li, Z.; Li, Y.; Yuan, Q. Ferriporphyrin-inspired MOFs as an artificial metalloenzyme for highly sensitive detection of H2O2 and glucose. *Chinese Chemical Letters* **2020**, *31*, 1398-1401, doi:10.1016/j.cclet.2020.03.052.

152. Shamsipur, M.; Safavi, A.; Mohammadpour, Z. Indirect colorimetric detection of glutathione based on its radical restoration ability using carbon nanodots as nanozymes. *Sensors and Actuators B: Chemical* **2014**, *199*, 463-469, doi:10.1016/j.snb.2014.04.006.
153. Chen, W.; Zhang, X.; Li, J.; Chen, L.; Wang, N.; Yu, S.; Li, G.; Xiong, L.; Ju, H. Colorimetric Detection of Nucleic Acids through Triplex-Hybridization Chain Reaction and DNA-Controlled Growth of Platinum Nanoparticles on Graphene Oxide. *Anal Chem* **2020**, *92*, 2714-2721, doi:10.1021/acs.analchem.9b04909.
154. Ding, W.; Song, C.; Li, T.; Ma, H.; Yao, Y.; Yao, C. TiO2 nanowires as an effective sensing platform for rapid fluorescence detection of single-stranded DNA and double-stranded DNA. *Talanta* **2019**, *199*, 442-448, doi:10.1016/j.talanta.2019.02.002.
155. Dioguardi, M.; Caloro, G.A.; Laino, L.; Alovisi, M.; Sovereto, D.; Crincoli, V.; Aiuto, R.; Coccia, E.; Troiano, G.; Lo Muzio, L. Circulating miR-21 as a Potential Biomarker for the Diagnosis of Oral Cancer: A Systematic Review with Meta-Analysis. *Cancers* **2020**, *12*, 936, doi:10.3390/cancers12040936.
156. Báez-Vega, P.M.; Echevarría Vargas, I.M.; Valiyeva, F.; Encarnación-Rosado, J.; Roman, A.; Flores, J.; Marcos-Martínez, M.J.; Vivas-Mejía, P.E. Targeting miR-21-3p inhibits proliferation and invasion of ovarian cancer cells. *Oncotarget* **2016**, *7*, 36321-36337, doi:10.18632/oncotarget.9216.
157. Liu, H.; Li, L.; Duan, L.; Wang, X.; Xie, Y.; Tong, L.; Wang, Q.; Tang, B. High Specific and Ultrasensitive Isothermal Detection of MicroRNA by Padlock Probe-Based Exponential Rolling Circle Amplification. *Analytical Chemistry* **2013**, *85*, 7941-7947, doi:10.1021/ac401715k.
158. Yu, N.; Wang, Z.; Wang, C.; Han, J.; Bu, H. Combining padlock exponential rolling circle amplification with CoFe2O4 magnetic nanoparticles for microRNA detection by nanoelectrocatalysis without a substrate. *Analytica Chimica Acta* **2017**, *962*, 24-31, doi:10.1016/j.aca.2017.01.069.
159. Mattiske, S.; Suetani, R.J.; Neilsen, P.M.; Callen, D.F. The Oncogenic Role of miR-155 in Breast Cancer. *Cancer Epidemiology, Biomarkers & Prevention* **2012**, *21*, 1236, doi:10.1158/1055-9965.EPI-12-0173.
160. Yang, M.; Shen, H.; Qiu, C.; Ni, Y.; Wang, L.; Dong, W.; Liao, Y.; Du, J. High expression of miR-21 and miR-155 predicts recurrence and unfavourable survival in non-small cell lung cancer. *European Journal of Cancer* **2013**, *49*, 604-615, doi:10.1016/j.ejca.2012.09.031.
161. Li, Q.; Liu, Z.; Zhou, D.; Pan, J.; Liu, C.; Chen, J. A cascade toehold-mediated strand displacement strategy for label-free and sensitive non-enzymatic recycling amplification detection of the HIV-1 gene. *Analyst* **2019**, *144*, 2173-2178, doi:10.1039/C8AN02340A.
162. Liang, Z.; Ou, D.; Sun, D.; Tong, Y.; Luo, H.; Chen, Z. Ultrasensitive biosensor for microRNA-155 using synergistically catalytic nanoprobe coupled with improved cascade strand displacement reaction. *Biosensors and Bioelectronics* **2019**, *146*, 111744, doi:10.1016/j.bios.2019.111744.
163. Wang, K.; Wu, C.; Wang, F.; Liao, M.; Jiang, G. Bimetallic nanoparticles decorated hollow nanoporous carbon framework as nanozyme biosensor for highly sensitive electrochemical sensing of uric acid. *Biosens Bioelectron* **2020**, *150*, 111869, doi:10.1016/j.bios.2019.111869.
164. Wang, Y.; Zhu, Y.; Binyam, A.; Liu, M.; Wu, Y.; Li, F. Discovering the enzyme mimetic activity of metal-organic framework (MOF) for label-free and colorimetric sensing of biomolecules. *Biosensors and Bioelectronics* **2016**, *86*, 432-438, doi:10.1016/j.bios.2016.06.036.
165. Gulba, D.C.; Barthels, M.; Westhoff-Bleck, M.; Jost, S.; Rafflenbeul, W.; Daniel, W.G.; Hecker, H.; Lichtlen, P.R. Increased thrombin levels during thrombolytic therapy in acute myocardial infarction. Relevance for the success of therapy. *Circulation* **1991**, *83*, 937-944, doi:10.1161/01.CIR.83.3.937.

166. Qu, Y.; Yang, Y.; Du, R.; Zhao, M. Peroxidase activities of gold nanowires synthesized by TMV as template and their application in detection of cancer cells. *Applied Microbiology and Biotechnology* **2020**, *104*, 3947-3957, doi:10.1007/s00253-020-10520-3.
167. Guo, J.; Zhao, X.; Hu, J.; Lin, Y.; Wang, Q. Tobacco Mosaic Virus with Peroxidase-Like Activity for Cancer Cell Detection through Colorimetric Assay. *Molecular Pharmaceutics* **2018**, *15*, 2946-2953, doi:10.1021/acs.molpharmaceut.7b00921.
168. Bruckman, M.A.; Czapar, A.E.; VanMeter, A.; Randolph, L.N.; Steinmetz, N.F. Tobacco mosaic virus-based protein nanoparticles and nanorods for chemotherapy delivery targeting breast cancer. *Journal of Controlled Release* **2016**, *231*, 103-113, doi:10.1016/j.jconrel.2016.02.045.
169. Kip, Ç.; Akbay, E.; Gökçal, B.; Savaş, B.O.; Onur, M.A.; Tuncel, A. Colorimetric determination of tumor cells via peroxidase-like activity of a cell internalizable nanozyme: Hyaluronic acid attached-silica microspheres containing accessible magnetite nanoparticles. *Colloids and Surfaces A: Physicochemical and Engineering Aspects* **2020**, *598*, 124812, doi:10.1016/j.colsurfa.2020.124812.
170. Alizadeh, N.; Salimi, A.; Hallaj, R.; Fathi, F.; Soleimani, F. Ni-hemin metal–organic framework with highly efficient peroxidase catalytic activity: toward colorimetric cancer cell detection and targeted therapeutics. *Journal of Nanobiotechnology* **2018**, *16*, 93, doi:10.1186/s12951-018-0421-7.
171. Liu, B.; Liu, J. Accelerating peroxidase mimicking nanozymes using DNA. *Nanoscale* **2015**, *7*, 13831-13835, doi:10.1039/c5nr04176g.
172. Qiu, S.; Wei, Y.; Tu, T.; Xiang, J.; Zhang, D.; Chen, Q.; Luo, L.; Lin, Z. Triazole-stabilized fluorescence sensor for highly selective detection of copper in tea and animal feed. *Food Chemistry* **2020**, *317*, 126434, doi:10.1016/j.foodchem.2020.126434.
173. Sharma, S.; Zapatero-Rodríguez, J.; Estrela, P.; Kennedy, R. Point-of-Care Diagnostics in Low Resource Settings: Present Status and Future Role of Microfluidics. *Biosensors* **2015**, *5*, 577-601, doi:10.3390/bios5030577.
174. Hayes, B.; Murphy, C.; Crawley, A.; O'Kennedy, R. Developments in Point-of-Care Diagnostic Technology for Cancer Detection. *Diagnostics* **2018**, *8*, 39, doi:10.3390/diagnostics8020039.
175. Fan, K.; Lin, Y.; Bansal, V. Editorial: Nanozymes: From Rational Design to Biomedical Applications. *Frontiers in chemistry* **2021**, *9*, 670767-670767, doi:10.3389/fchem.2021.670767.
176. Li, R.; Zhang, L.; Wang, P. Rational design of nanomaterials for water treatment. *Nanoscale* **2015**, *7*, 17167-17194, doi:10.1039/c5nr04870b.
177. Liu, R.; Priestley, R.D. Rational design and fabrication of core–shell nanoparticles through a one-step/pot strategy. *Journal of Materials Chemistry A* **2016**, *4*, 6680-6692.
178. Raveendran, M.; Lee, A.J.; Sharma, R.; Wälti, C.; Actis, P. Rational design of DNA nanostructures for single molecule biosensing. *Nat Commun* **2020**, *11*, 4384, doi:10.1038/s41467-020-18132-1.
179. Kanekiyo, M.; Bu, W.; Joyce, M.G.; Meng, G.; Whittle, J.R.; Baxa, U.; Yamamoto, T.; Narpala, S.; Todd, J.P.; Rao, S.S., et al. Rational Design of an Epstein-Barr Virus Vaccine Targeting the Receptor-Binding Site. *Cell* **2015**, *162*, 1090-1100, doi:10.1016/j.cell.2015.07.043.
180. Lew, T.T.S.; Wong, M.H.; Kwak, S.Y.; Sinclair, R.; Koman, V.B.; Strano, M.S. Rational Design Principles for the Transport and Subcellular Distribution of Nanomaterials into Plant Protoplasts. *Small (Weinheim an der Bergstrasse, Germany)* **2018**, *14*, e1802086, doi:10.1002/smll.201802086.
181. Wang, Q.; Li, Q.; Lu, Y.; Zhang, X.; Huang, Y. Rational Design of N-Doped Carbon Nanocage-Equipped Co-Nx Active Sites for Oxidase Mimicking and Sensing Applications. *ACS Sustainable Chemistry & Engineering* **2021**, *9*, 7668-7677, doi:10.1021/acssuschemeng.1c02635.
182. Liu, Y.; Qin, Y.; Zhang, Q.; Zou, W.; Jin, L.; Guo, R. Arginine-rich peptide/platinum hybrid colloid nanoparticle cluster: a single nanozyme mimicking multi-enzymatic cascade systems in peroxisome. *Journal of Colloid and Interface Science* **2021**.

183. Geng, R.; Chang, R.; Zou, Q.; Shen, G.; Jiao, T.; Yan, X. Biomimetic Nanozymes Based on Coassembly of Amino Acid and Hemin for Catalytic Oxidation and Sensing of Biomolecules. *Small (Weinheim an der Bergstrasse, Germany)* **2021**, *17*, 2008114, doi:10.1002/smll.202008114.